Institute of Space and Aeronautical Science, University of Tokyo
Report No. 590, February 1981

Heat Transfer from Cylinder and Plate in Large-Amplitude Oscillating Flows

By

Susumu KOTAKE and Isao AOKI

Summary: The heat transfer characteristics of a flat plate, a cylinder and a cylinder above a flat plate located in sinusoidally oscillating flows with large amplitudes were investigated experimentally by measuring the velocity and temperature distributions and the wall-temperature oscillation. The time-mean values are hardly affected by the velocity oscillation. The amplitude of their oscillation is rapidly reduced from the quasi-steady value to vanishing values with increasing the frequency of velocity oscillation. The phase advances from 180° lag to be in-phase at higher frequencies. These features are more remarkable in the inner part of the boundary layer than in the outer layer.

CONTENTS

NOMENCLATURE

A surface area of heater (m^2)

c	specific heat (kcal/kg°C)
d	diameter of cylinder (mm)
f	frequency (Hz)
H	distance between cylinder and plate (mm)
h	heat transfer coefficient, q/θ_w (kcal/m²h°C)
N_u	Nusselt number, hx/λ, hd/λ
R_e	Reynolds number, $U_\infty x/\nu$, $U_\infty d/\nu$
Q	overall heat flux, qA (kcal/h)
q	heat flux per unit surface area, Q/A (kcal/m²h)
T	temperature (°C)
t	time (s)
t_w	thickness of heater foil (mm)
U, V	flow velocity components (m/s)
u, v	turbulent velocity components (m/s)
x, y	coordinates (mm)
α_u	amplitude of velocity oscillation
α_t	amplitude of temperature oscillation
α_{hm}	$=\Delta\theta_{wm}/\bar{\theta}_{wm}$
Δ	oscillating component
ΔU	$=U_{\max}-U_{\min}$ (m/s)
$\Delta\theta$	$=\theta_{\max}-\theta_{\min}$ (degC)
δ	phase difference
θ	excess temperature, $T-T_\infty$ (degC)
λ	heat conductivity (kcal/mh°C)
ρ	density (kg/m³)
ω	angular frequency (rad/s)
Superscript	
—	time mean
Subscripts	
m	average over wall-surface
t	temperature
u	velocity
w	wall surface
∞	main flow

1. Introduction

The convective heat transfer problems of unsteady or oscillating flows are often encountered in engineering practice of thermal systems such as reciprocating machineries, gas turbines and rocket motors. The knowledge of the heat transfer in unsteady flows is of the most importance for considering the thermal reliability and safety as well as for estimating the unsteady performance of the system. For example, in a highly rated combustion system, heat transfer rates increased locally in space or time due to unsteady flows could well lead to the failure of certain com-

ponents of which the critical temperature has been computed from the steady-flow heat transfer.

Although, concerning the unsteady-flow heat transfer, much work has been published, it appears to have been confined to problems of internal flows such as pipe and channel flows and of external flows with small amplitudes. For the latter, much theoretical work has also been done with the perturbation theory [*1* ~ *5*]. The predicted effects of velocity oscillation are so small as to be detectable [*6*]. On the other hand, enhanced heat transfer rates with oscillating external flows have been observed [*7*, *8*], although these discordant results would be explained by the unidentified gross flow behavior such as flow instabilities and flow structures.

It is felt, however, from the standpoint of practical engineering that the need remains for the knowledge of heat transfer rates from a body in oscillating or pulsating flows with large amplitudes. The oscillating flow would affect both the positions of laminar-turbulent transition and separation and the structure of turbulent flow. Large amplitudes of velocity oscillation could change the boundary layer flow close to the body surface from laminar to turbulent and from turbulent to laminar periodically. The rate of heat transfer from the body surface takes higher values in turbulent flows than in laminar flows. If separation occurs at certain times of the period, the flow undergoes separation and reattachment alternately. At separation, the heat transfer rate is greatly reduced, and it is enchanced by the reattachment of flow. Velocity oscillation may change the process of the turbulent-energy production, hence the structure of turbulence which controls the convective heat transfer.

As a fundamental research for such a problem, it is the object of the present study to investigate experimentally the heat transfer characteristics of a cylinder, a flat plate and a cylinder-and-plate system in oscillating flows with large amplitude. A wind tunnel was equipped to supply air flows with exactly sinusoidally oscillation at high amplitudes. A cylinder and/or a plate heated electrically were located in the oscillating flows. The velocity and temperature distributions in space and time were measured to obtain the heat transfer characteristics.

2. Experimental apparatus and procedures

2–1 *Experimental apparatus*

Air flow of varying velocity in time can be obtained by several methods, such as changing the source pressure and temperature, bypassing a part of flow, or altering the cross-sectional area of flow passage. The latest is the simplest and the most precise method for realizing the required flows. The variation of the cross-sectional area of flow passage is usually associated with the change in the flow resistance so that the flow velocity does not have a linear response to the change in the cross-sectional area. In addition, it is not always easy to alter the cross-section mechanically. In order to solve such problems, we devised a method of two "choked throats" located at the outlet from the air stroage tank which produced changes in the cross-sectional area alternately in anti-phase as shown in Fig. 2–1 [*9*]. By this means, the pressure

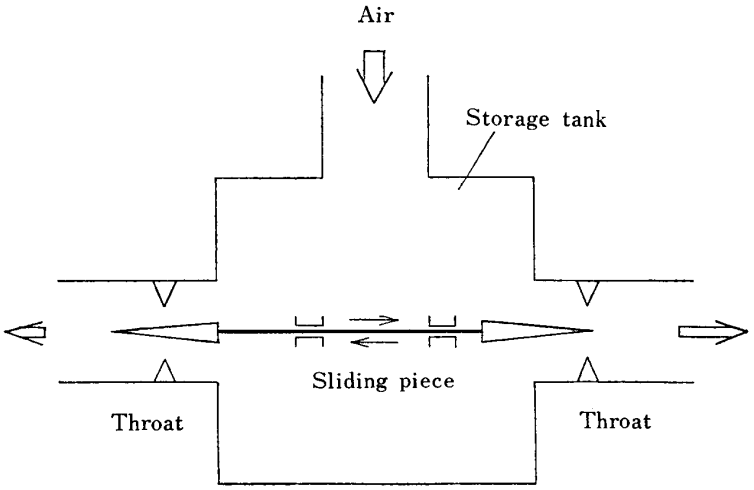

FIG. 2-1. Principle of chaning flow velocity.

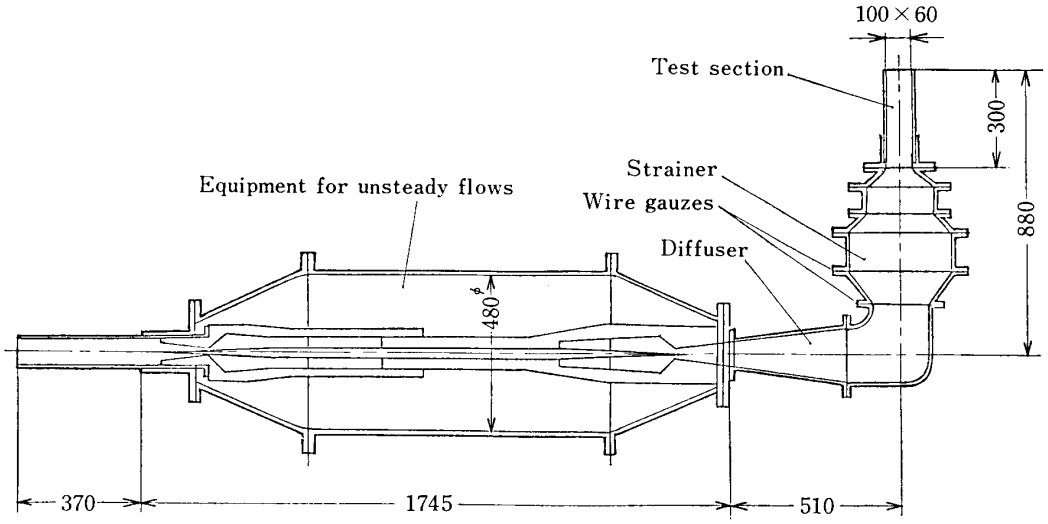

FIG. 2-2. Unsteady wind tunnel.

in the storage tank can be kept constant, regardless of the change in the cross-sectional area of the throat, and constant amount of air mass with respect to time can be introduced into the tank. Then, the mean flow velocity through the throat has a linear response to the change in the throat area, which facilitates the design of the mechanical configuration required for the variation of the area; simply two geometrically symmetrical throats.

In the present apparatus, the throat area is changed by a sliding motion of a wedge-shaped piece of brass through the throat. The air stored in the tank is released from the one of throats into the surroundings and from the other one into the test section through a diffuser and a strainer as shown in Fig. 2-2. The test section is placed vertically to avoid the influence of natural convection. The test section has a cross-sectional area of $60 \times 100\,\mathrm{mm}^2$ and a length of 300 mm, being assembled of heat-insulating materials 15 mm thick.

The outline of the overall equipment is shown in Fig. 2.3. The high pressure air

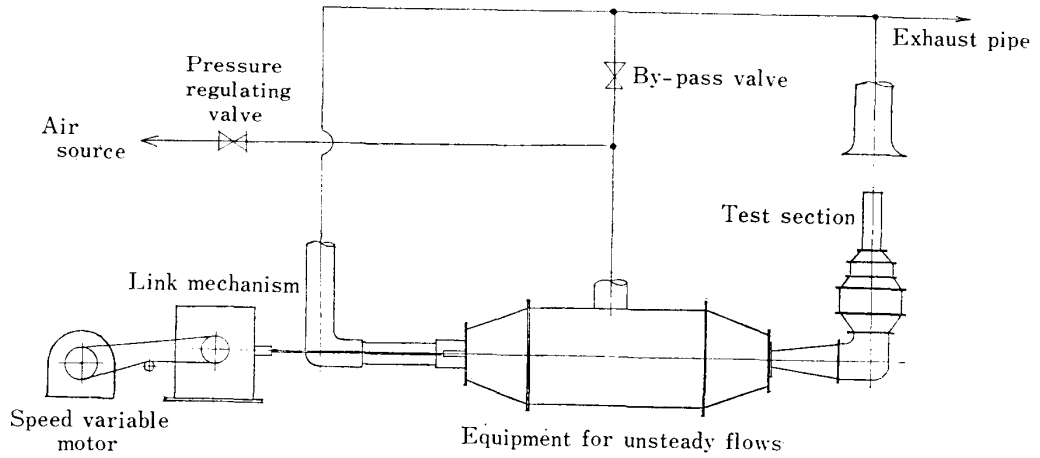

FIG. 2-3. Unsteady wind tunnel equipment.

with regulated temperature and humidity is introduced from a high pressure storage tank into the equipment through pressure-regulators. The sliding piece is driven by a cam and link mechanism, the Scotch York link mechanism which transforms a circular motion into an exactly sinusoidal rectilinear motion projected onto the diameter of the circle. The detailed performance of the equipment was reported in Ref. 9. It can provide exactly sinusoidally oscillating flows of velocities $0 \sim 60$ m/s and amplitudes up to 80% at 3 Hz and 10% at 10 Hz. The flow velocity is uniform throughout above 80% of the test area. The intensity of turbulence is hardly altered by changing the frequency, amplitude or mean velocity of flow.

2-2 *Experimental procedures*

Using the equipment mentioned above, we investigated the heat-transfer characteristics of a flat plate, a cylinder and a cylinder-above-plate located in sinusoidally oscillating air-flows with large amplitudes. Used plates and cylinders are described in the next chapter. The heated walls were obtained by directly heating a thin stainless steel foil of 15 to 200 μm thick. Temperatures of the wall surface and of air in the boundary layer of the wall were measured by copper-constantan thermocouples of 18 μm in diameter of which the thermal time constant in the heated air ($d_c^2 \rho_c c_c / \lambda_{air}$) was about 3×10^{-3} sec, hence it had a sufficient response to follow the temperature oscillations encountered in the present experiment ($f_{\max}^{-1} \simeq 0.1$ sec). Flow velocities and their turbulence intensities were measured by a 5 μm hotwire constant-temperature anemometer. The heat fluxes through the wall were calculated from the applied electric power to the thin stainless steel foil. The measurement system used in the experiment is shown in Fig. 2-4.

Corresponding to the specified mean-velocity and amplitude of the main flow, the relative positions of the two throats were first determined. The amplitude and frequency of the link mechanism were set to obtain the specified flow. By opening the valve of the air source, adjusting the valve of the pressure regulator and by-passing the air, the pressure in the air storage tank was set so as to choke the throats throughout the oscillation. After heating the stainless-steel foil, the link mechanism was

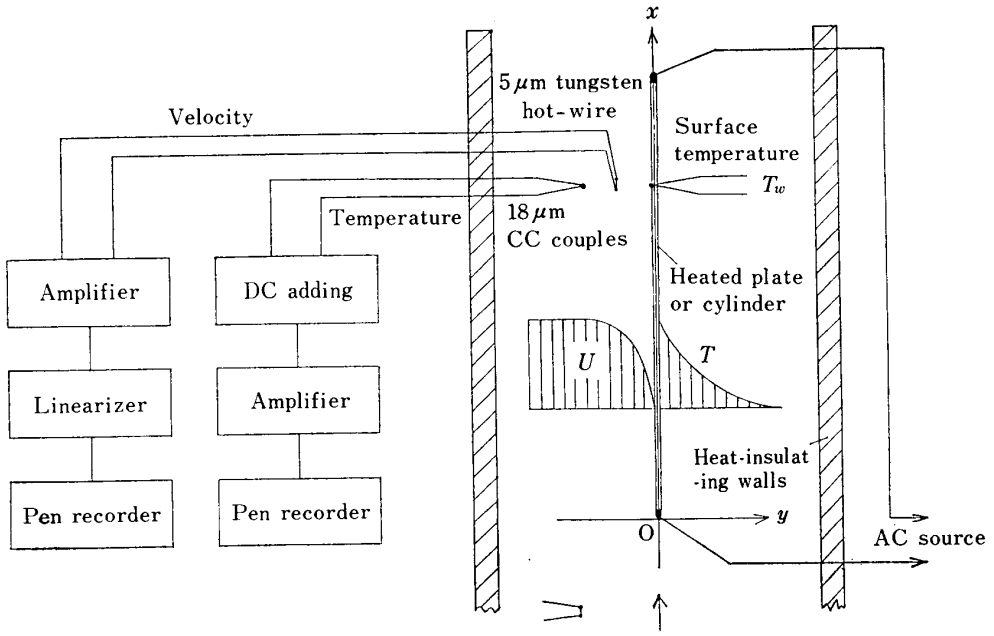

FIG. 2–4. Heat transfer apparatus and measurement system.

set in motion. Thermal equilibrium had been attained before the experimental measurements described above were started.

The main oscillating flows obtained by the present equipment can be expressed as

$$U_\infty = \overline{U}_\infty(1+\alpha_{u\infty}\sin\omega t), \tag{2-1}$$

where $\overline{U}_\infty$ is the time-mean of the main flow velocity, $\alpha_{u\infty}\overline{U}_\infty$ the amplitude of the oscillating velocity, and ω the angular velocity

$$\omega = 2\pi f \qquad (f\text{: frequency}).$$

The velocity and temperature associated with the oscillating main flow can be expressed in the form of

$$U = \overline{U}\{1+\alpha_u \sin(\omega t+\delta_u)\} = \overline{U} + \frac{\Delta U}{2}\sin(\omega t+\delta_u) \tag{2-2}$$

$$\theta = \bar{\theta}\{1+\alpha_t \sin(\omega t+\delta_t)\} = \bar{\theta} + \frac{\Delta\theta}{2}\sin(\omega t+\delta_t) \tag{2-3}$$

where θ is the temperature referred to the temperature of the oncoming flow

$$\theta = T - T_\infty. \tag{2-4}$$

$\overline{U}$ and $\bar{\theta}$ are the time-mean velocity amd temperature, and α_u and α_t are the amplitude fraction of velocity and temperature, respectively. δ_u and δ_t mean their phase difference with respect to the main-flow velocity. α_u, α_t, δ_u and δ_t are a function of the measuring position. ΔU and $\Delta\theta$ are the difference between the maximum and minimum of velocity and temperature, respectively

$$\begin{aligned} \Delta U &= U_{\max} - U_{\min} \\ \Delta\theta &= \theta_{\max} - \theta_{\min}. \end{aligned} \tag{2-5}$$

The wall temperature is written as

$$\theta_w = \bar{\theta}_w\{1 + \alpha_{tw} \sin(\omega t + \delta_{tw})\} = \bar{\theta}_w + \frac{\Delta\theta_w}{2} \sin(\omega t + \delta_{tw}). \tag{2-6}$$

Strictly speaking, the associated velocity and temperature may have the higher harmonics other than the fundamental frequency, $\sin(n\omega t + \delta)$, $n = 2, 3, 4, \cdots$. As mentioned in Ref. 9 , the higher harmonics were hardly recognized in the observed velocity and temperature distributions, hence it was easy to find the amplitudes, α_u and α_t, and the phase differences, δ_u and δ_t from the records of the time-history of velocity and temperature.

With the measured wall temperatures, the heat transfer coefficients can be calculated. The heat released by electrically heating the wall plate per unit area and unit time, q, is consumed to heat up the plate itself and the air flow adjacent to the wall;

$$q = \rho_w c_w t_w \frac{\partial\theta_w}{\partial t} - \lambda\left(\frac{\partial\theta}{\partial y}\right)_{y=0} \tag{2-7}$$

where ρ_w is the density of the plate material, c_w its specific heat, t_w the thickness of the wall plate and λ the heat conductivity of air. The heat transfer coefficient of the wall plate can be defined as

$$h\theta_w = -\lambda\left(\frac{\partial\theta}{\partial y}\right)_{y=0}, \tag{2-8}$$

that is,

$$h = \frac{q - \rho_w c_w t_w (\partial\theta_w/\partial t)}{\theta_w}. \tag{2-9}$$

By using the sinusoidal expression of the wall temperature, it can be rewritten

$$h = \frac{q - (1/2)\rho_w c_w t_w \omega \Delta\theta_w \cos(\omega t + \delta_{tw})}{\bar{\theta}_w + (1/2)\Delta\theta_w \sin(\omega t + \delta_{tw})}, \tag{2-10}$$

where the plate is assumed to have a uniform temperature equal to the wall surface temperature.

The time-mean heat transfer coefficient is then

$$\bar{h} = \frac{q}{\bar{\theta}_w}. \tag{2-11}$$

If the heat transfer coefficient is expressed as

$$h = \bar{h} + \Delta h(t), \tag{2-12}$$

the variation term with respect to time, $\Delta h(t)$, can be given by

$$\Delta h(t) = -\frac{\bar{h}\sin(\omega t+\delta_{tw})+\rho_w c_w t_w \omega \cos(\omega t+\delta_{tw})}{1+(\Delta\theta_w/2\bar{\theta}_w)\sin(\omega t+\delta_{tw})}\frac{\Delta\theta_w}{2\bar{\theta}_w}. \tag{2-13}$$

For $\Delta\theta_w/\theta_w \ll 1$,

$$\Delta h(t) = -\bar{h}\frac{\Delta\theta_w}{2\bar{\theta}_w}\sqrt{1+\left(\frac{\rho_w c_w t_w \omega}{\bar{h}}\right)^2}\sin(\omega t+\delta_h), \tag{2-14}$$

$$\tan(\delta_h-\delta_{tw}) \equiv \frac{\rho_w c_w t_w \omega}{\bar{h}}.$$

Further, depending on the value of $\rho_w c_w t_w \omega/\bar{h}$, the above relation is reduced to

$$|\Delta h(t)| = \begin{cases} \dfrac{\rho_w c_w t_w \omega}{2}\dfrac{\Delta\theta_w}{\bar{\theta}_w} & \dfrac{\rho_w c_w t_w \omega}{\bar{h}} \gg 1 \\ \dfrac{\bar{h}}{2}\dfrac{\Delta\theta_w}{\bar{\theta}_w} & \dfrac{\rho_w c_w t_w \omega}{\bar{h}} \ll 1. \end{cases} \tag{2-15}$$

3. Heat transfer from a flat plate in oscillating flows

A heated flat plate was located in oscillating air flows, and the air temperatures in the boundary layer of the plate and the wall temperatures were measured to investigate the heat transfer characteristics of the plate. The plate was constructed from a bakelite plate 2 mm thick, 59 mm wide and 215 mm long covered with a thin stainless-steel foil of 15, 20, 50 μm thick shown in Fig. 3–1. Both leading and trailing edges of the plate were made of copper to act as the electrodes for directly electrically heating the stainless-steel foil. The heated foil was kept stretched by springs inserted between the copper edge and the bakelite plate. Wall temperatures of the heated plate were measured by copper-constantan thermocouples of 18 μm in diameter soldered to the foil.

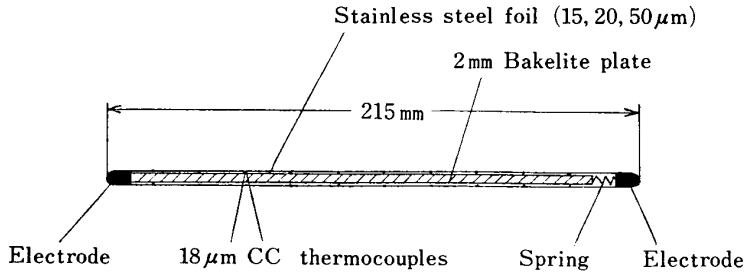

Fig. 3–1. Heated flat plate.

3–1 *Velocity distribution*

Since the variation of physical quantities with respect to temperature is sufficiently negligible for the case of small heat fluxes employed to the heated plate, the velocity distribution in the heated boundary layer can be regarded to concide with the one in the unheated layer. The velocity distribution in the boundary layer of the plate

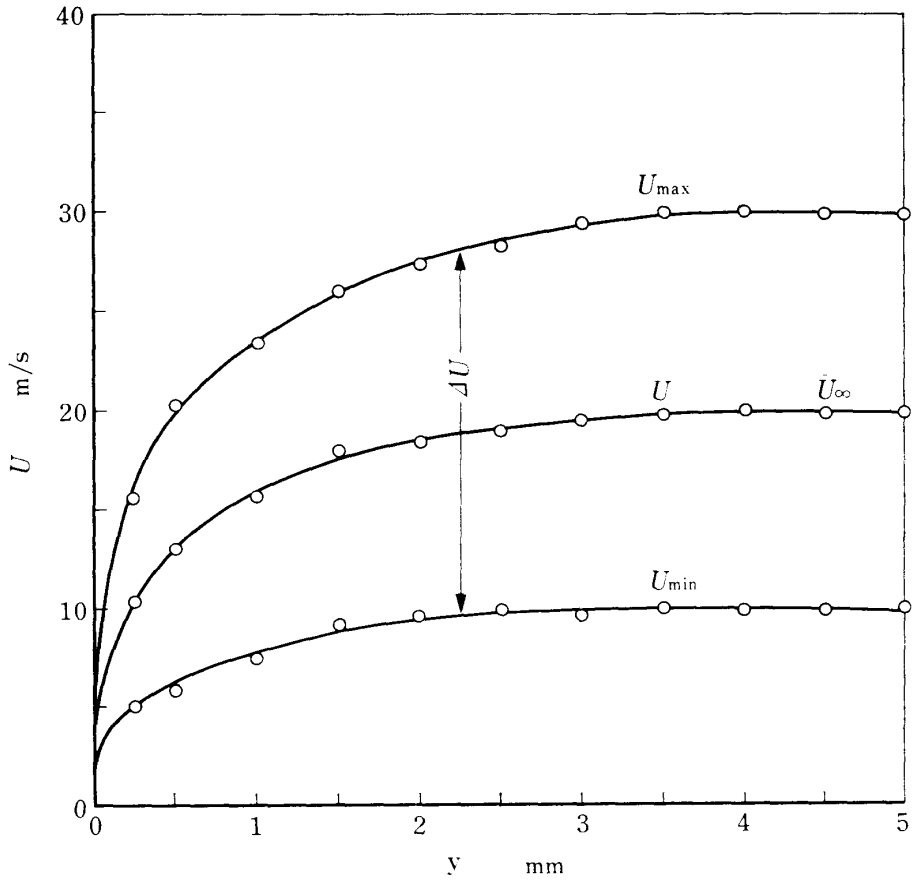

FIG. 3–2. Velocity distribution in the boundary layer of the plate; $\bar{U}_\infty=20$ m/s, $a_{u\infty}=0.5$, $f=1.0$ Hz, $x=162$ mm.

was measured only in the case of unheated flows with a 5 μm tungsten hot-wire anemometer.

In Fig. 3–2, a typical velocity distribution in the boundary layer is shown for its maximum U_{max}, minimum U_{min}, and time-mean values $\bar{U}$. The abscisa y means the distance measured perpendicularly from the surface of the plate. A typical example of the time-history of velocity is shown in Fig. 3–3. It has scarcely higher harmonics and can be expressed by Eq. (2–2). The amplitude of velocity decreases as close to the plate wall. The velocity has no phase difference at any position within the layer for flows of frequencies, amplitudes and mean velocities in the range of the present experimeent. The amplitude of the associated velocity in the boundary layer is shown in Fig. 3–4. In the inner part of the layer, the velocity has relatively larger amplitudes compared with the one in the outer part. This may be attributed to the small inertia of the fluid of slow motion in the inner part. Further, in the inner part of the layer, the higher frequency oscillation results in larger amplitudes of velocity, whereas in the outer part it yields smaller amplitudes.

The turbulent intensities, $\overline{u^2}$ and $\overline{v^2}$, and the Reynolds stress, $\overline{uv}$ are shown in Fig. 3–5. They are not considerably affected by velocity oscillation. In the outer part of the boundary layer, they are slightly increased whereas in the inner layer they are likely to be decreased. On the frequency spectra of the turbulent properties in the

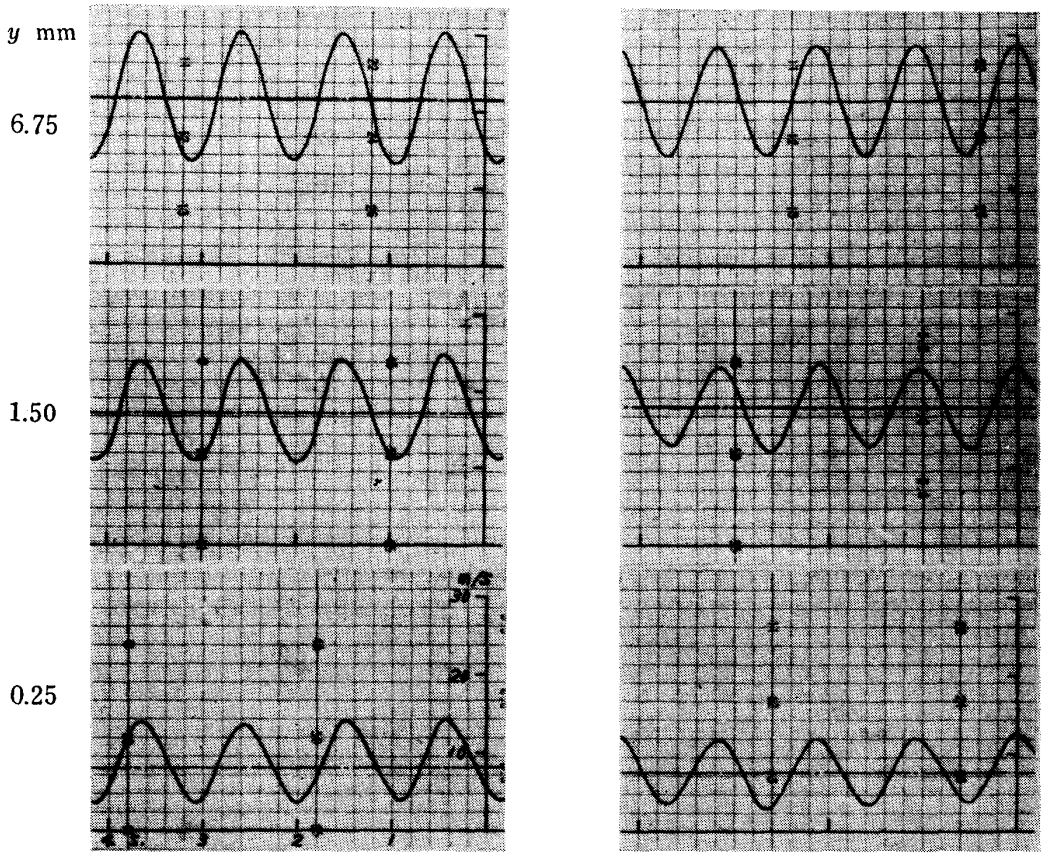

FIG. 3-3. Time histories of velocity oscillation; $\overline{U}_\infty = 20$ m/s, $\alpha_{u\infty} = 0.4$, $x = 162$ mm.

inner layer, however, velocity oscillations are found to have little effect.

3-2 *Temperature distribution*

Typical records of temperature oscillation in the boundary layer are shown in Fig. 3-6. It can also be expressed by Eq. (2-3), having little higher harmonics. The bottom trace is the main velocity. Time origins of the figure are identical in order to clarify their phase relation. The amplitude of temperature decreases rapidly with increasing the distance from the plate wall. The phase of temperature lags by about 90° with respect to the main flow velocity.

The experiment was carried out for various test conditions of

velocity oscillation:	$\overline{U}_\infty = 10 \sim 40$ m/s, $\alpha_{u\infty} = 0 \sim 0.5$, $f = 0 \sim 5$ Hz,
heat flux:	$q = 10^3 \sim 10^5$ kcal/m²h,
heater thickness:	$t_w = 15, 20, 50$ μm.

In the following illustration of the results, a typical condition is selected;

$$\overline{U}_\infty = 30 \text{ m/s}, \quad \alpha_{u\infty} = 0.5, \quad f = 1.0 \text{ Hz}, \quad t_w = 15 \ \mu\text{m}, \quad q = 5071 \text{ kcal/m}^2\text{h}.$$

The time-means of temperature distribution in the boundary layer are shown in

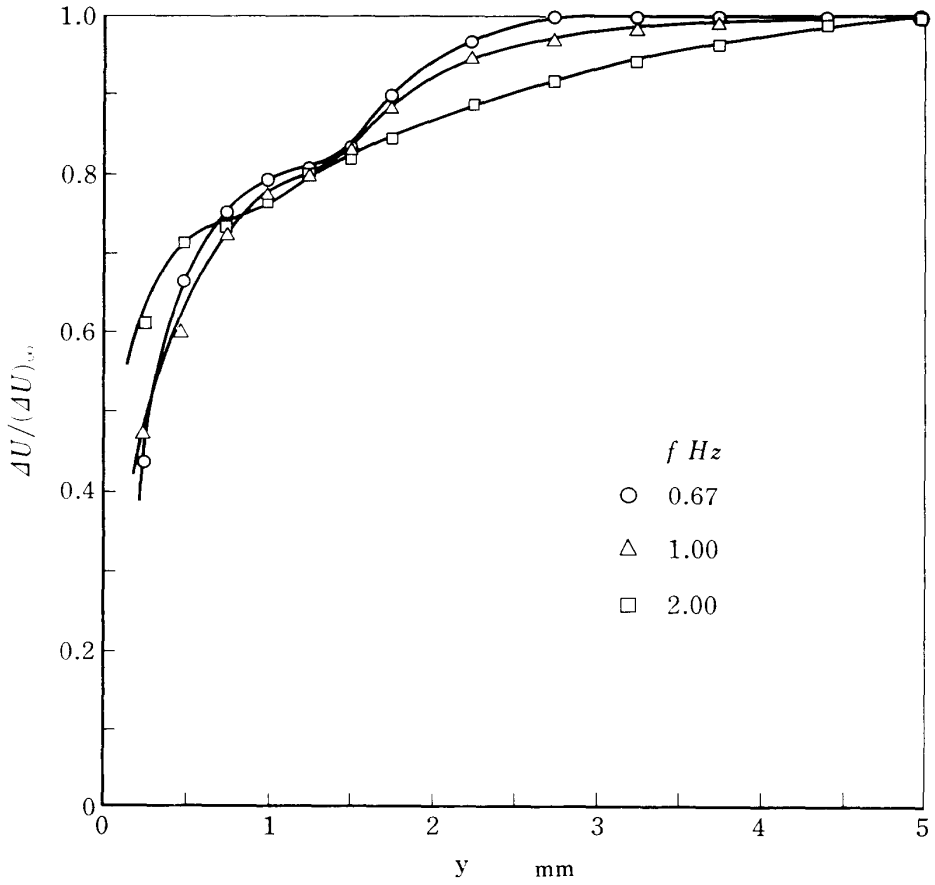

FIG. 3–4. Amplitude of velocity oscillation in the boundary layer; $\bar{U}_\infty=20$ m/s, $\alpha_{u\infty}=0.5$, $x=162$ mm.

Fig. 3–7. For the constant heat flux through the wall, the time-mean temperatures in the layer are hardly affected by the velocity oscillation. The effect of the frequency and amplitude of velocity oscillation on the time-mean temperature is shown in Fig. 3–8. It is very interesting that such large changes in velocity field have little influence upon the temperature field in the time-mean scale.

Figure 3–9 shows the amplitude distribution of temperature oscillation in the boundary layer. As the frequency of velocity oscillation increases, the amplitude of temperature oscillation decreases rapidly through the layer. The amplitude of velocity oscillation increases approximately linearly the amplitude of temperature oscillation at all parts of the layer. As closer to the wall, the amplitude increases at first proportionally to the time-mean temperature and then decreases after taking a maximum in the inner layer. The phase of temperature oscillation always advances in the inner layer compared with that in the main flow as shown in Fig. 3–10. These show that, in the inner layer close to the wall, the slow moving fluid would result in the forced convection (phase advance) overcoming the thermal inertia (phase lag) due to its rapid response to the acceleration force of velocity oscillation. The phase of temperature oscillation advances throughout the layer as the frequency of velocity oscillation increases. It should lag by 180° for quasi-steady flows. The amplitude of velocity

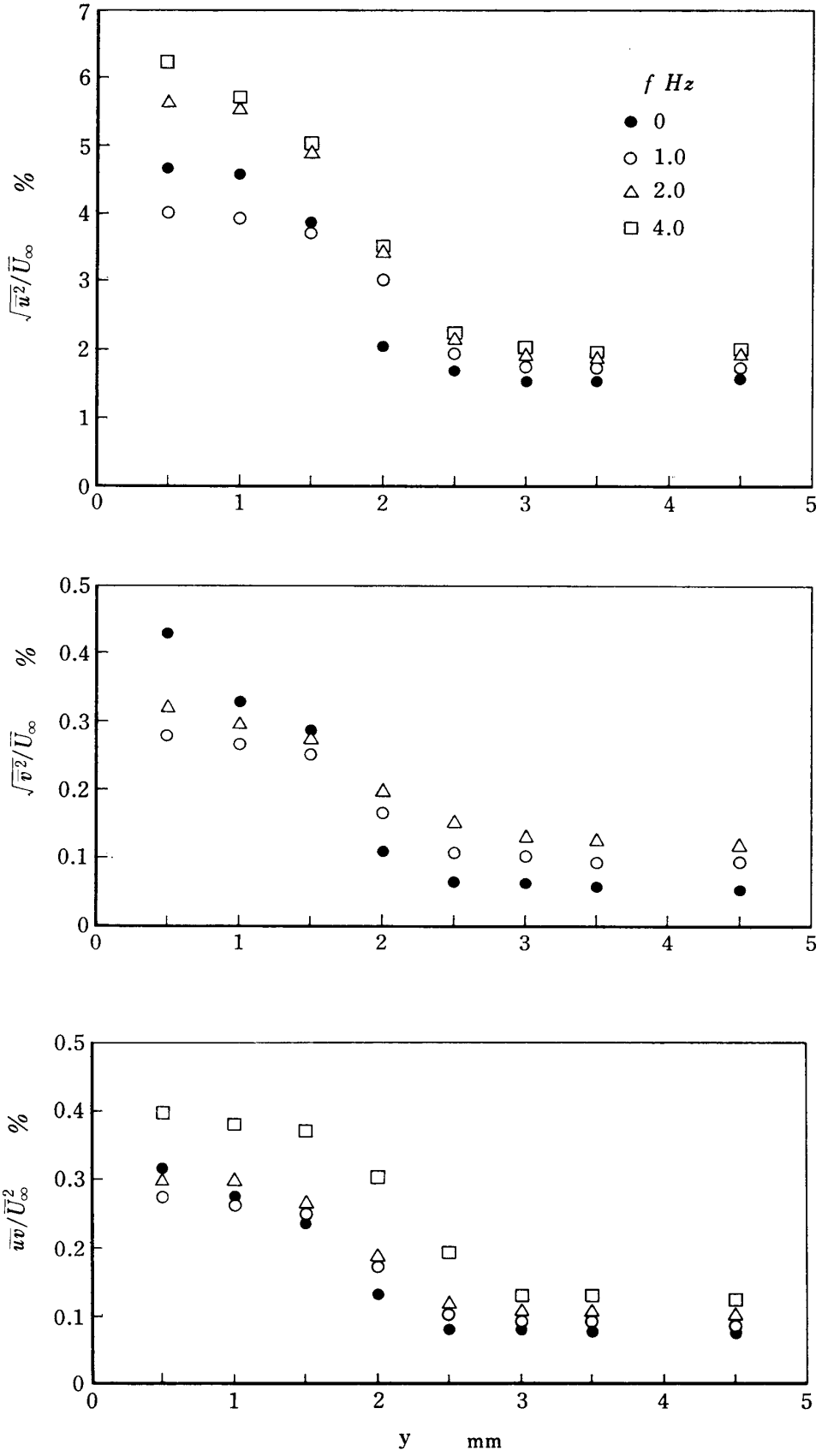

(a) Effect of frequency

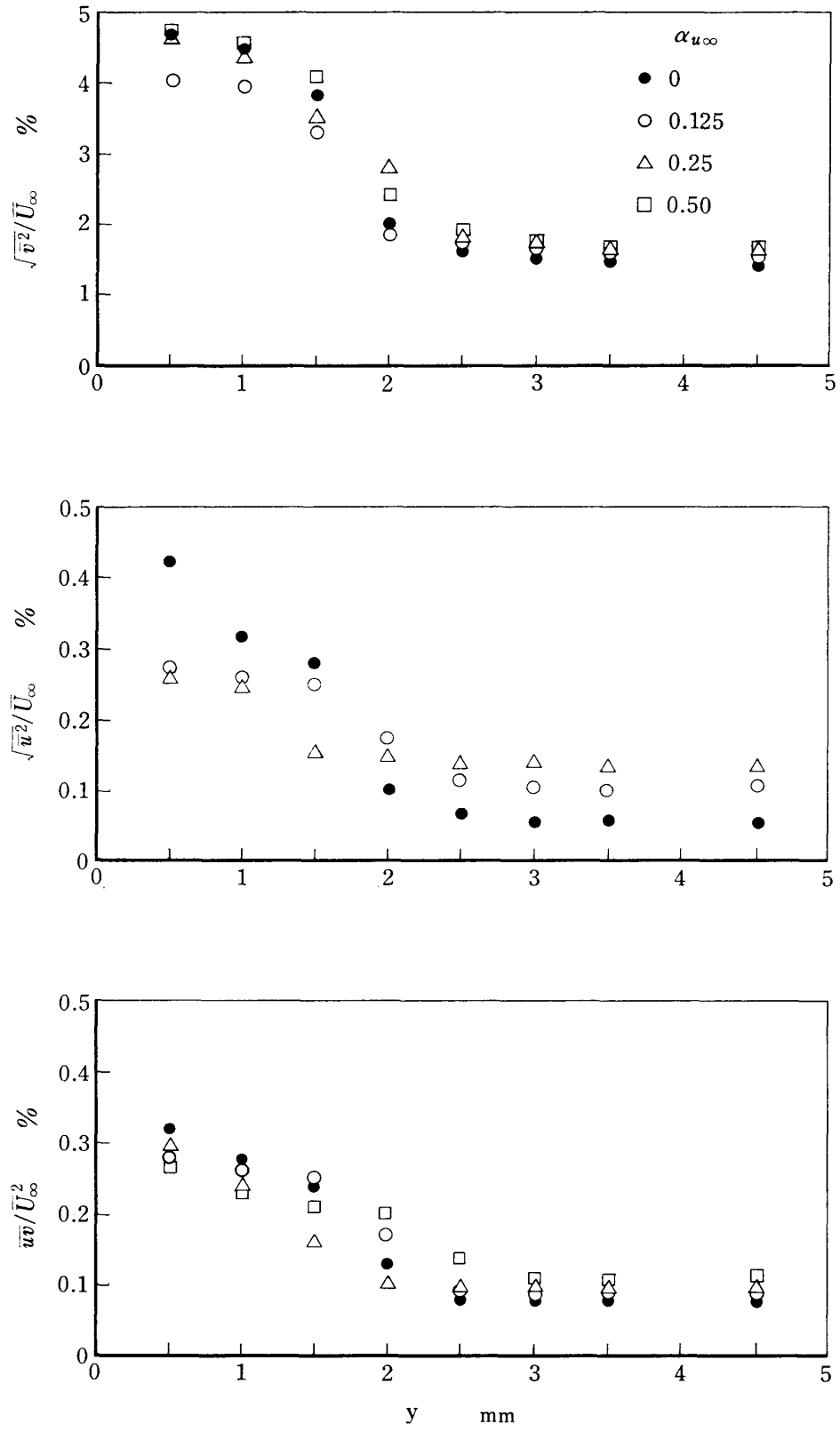

(b) Effect of amplitude

FIG. 3-5. Turbulent velocity distributions $\sqrt{\overline{u^2}}/\overline{U}_\infty$, $\sqrt{\overline{v^2}}/\overline{U}_\infty$ and $\overline{uv}/\overline{U}_\infty$; $\overline{U}_\infty=$ 30 m/s, $\alpha_{u\infty}=0.125$ (a), $f=1.0$ Hz (b), $x=105$ mm.

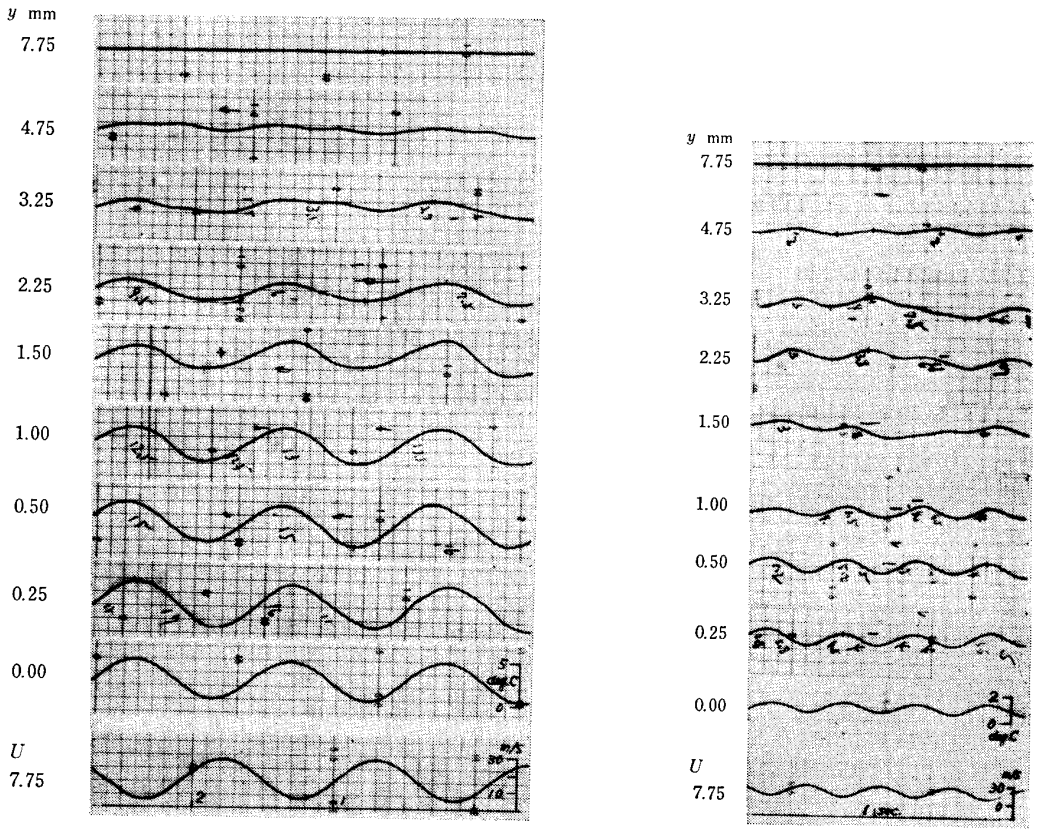

$f=1.0$ Hz $f=2.0$ Hz

FIG. 3–6. Time histories of temperature oscillation in the boundary layer; $\bar{U}_\infty=20$ m/s, $\alpha_{u\infty}=0.6$, $x=162$ mm, $t_w=15$ μm, $q=3360$ kcal/m^{2}h.

oscillation as well as the thickness of the heated foil has no effect on the phase relations between velocity and temperature oscillations.

3–3 *Heat transfer characteristics*

In Figs. 3–11 to 3–16, the time-mean value, amplitude and phase difference of the wall temperature are shown along the mean flow direction parallel to the plate where the x coordinate is measured from the leading edge of the plate.

The time-mean values of wall temperature are hardly affected by both frequency and amplitude of velocity oscillation as seen in Fig. 3–12. This leads to no effect of velocity oscillation on the characteristics of time-mean heat transfer of the plate. The dimensionless heat-transfer coefficient, that is, the Nusselt number is defined by

$$N_u=\frac{hx}{\lambda}.$$

The time-mean Nusselt number is then

$$\bar{N}_u=\frac{\bar{h}x}{\lambda}.$$

The observed result shows that velocity oscillations could not make any change in

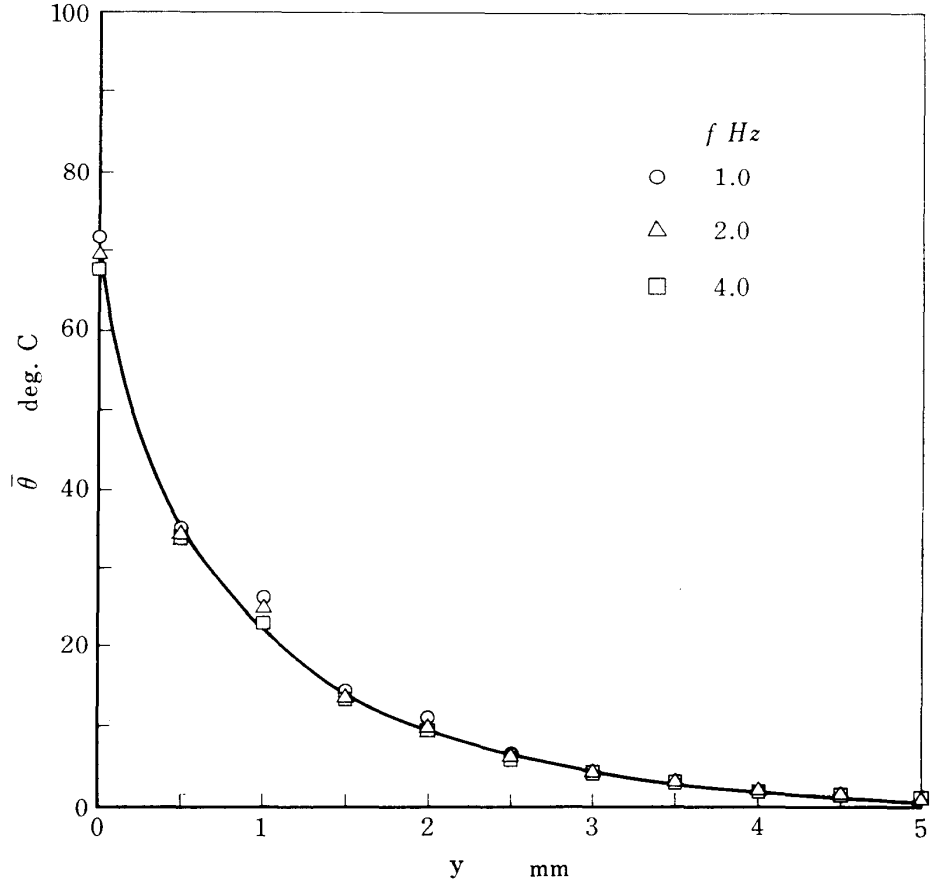

FIG. 3-7. Time-mean temperature distribution in the boundary layer; $\bar{U}_\infty=30$ m/s, $\alpha_{u\infty}=0.083$, $x=143$ mm, $t_w=15$ μm, $q=5071$ kcal/m²h.

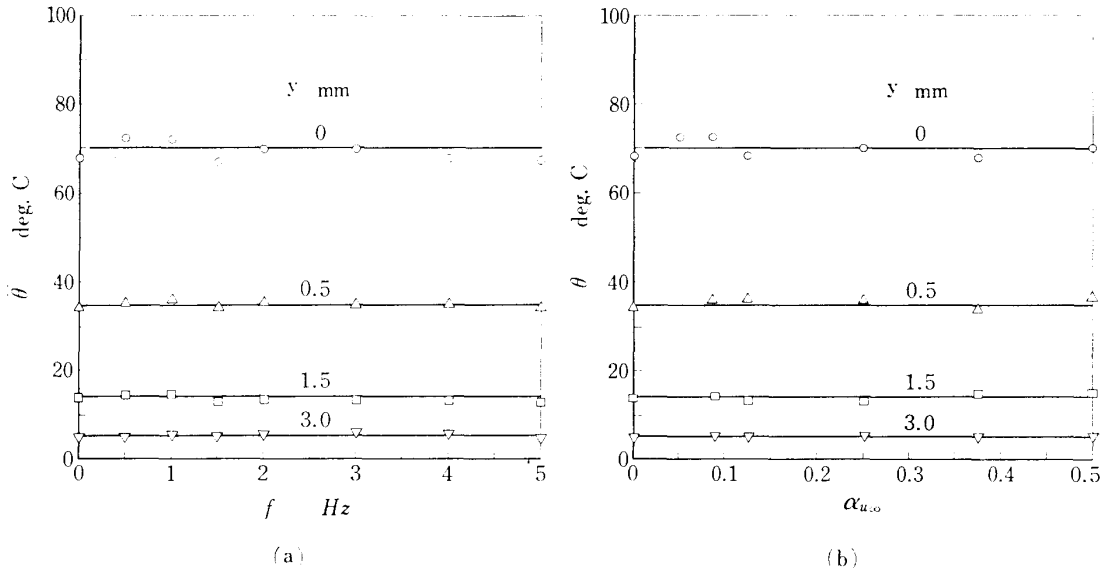

FIG. 3-8. Effect of frequency and amplitude of velocity oscillation on the time-mean temperature in the boundary layer; $\bar{U}_\infty=30$ m/s, $\alpha_{u\infty}=0.083$(a), $f=1.0$ Hz(b), $x=143$ mm, $t_w=15$ μm, $q=5071$ kcal/m²h.

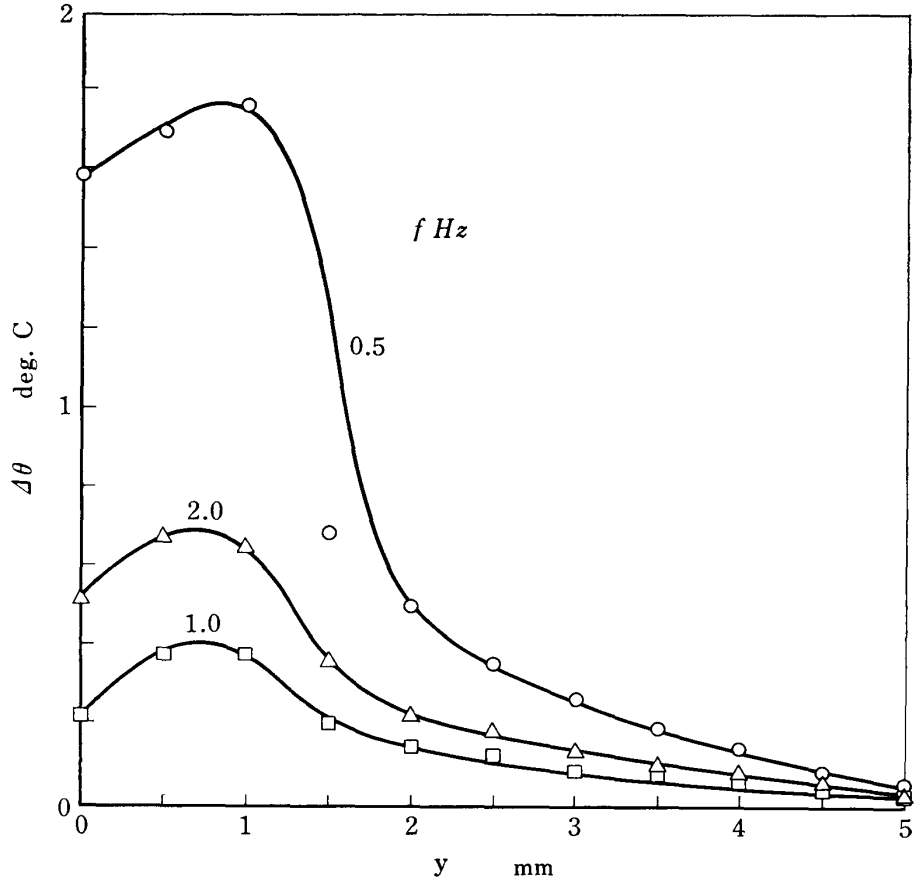

(a)

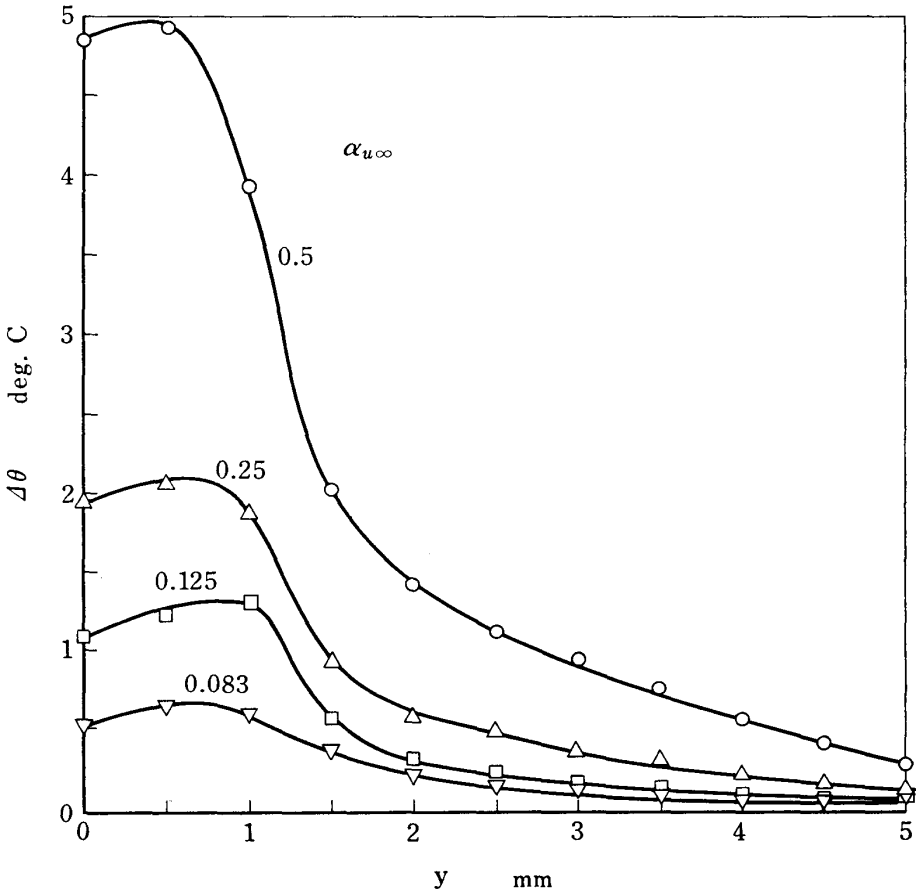

(b)

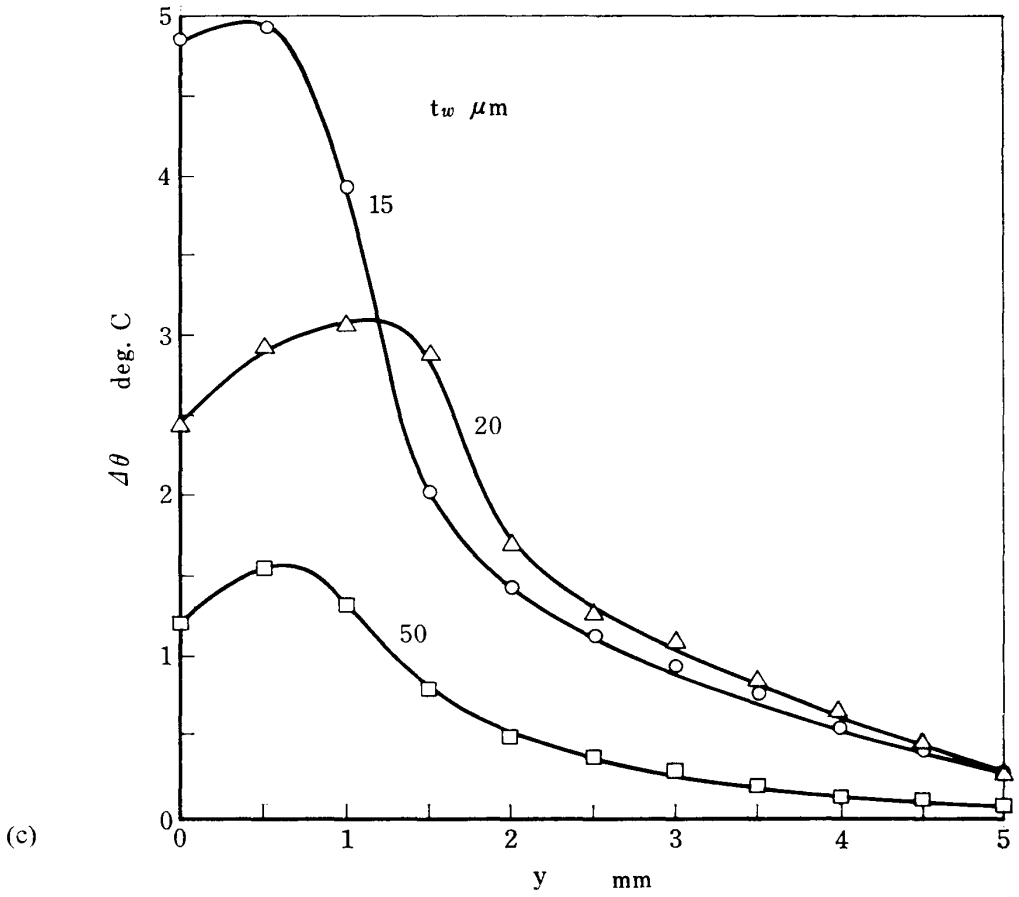

(c)

FIG. 3-9. Amplitude distribution of temperature oscillation in the boundary layer; $\bar{U}_\infty=30$ m/s, $x=143$ mm, $q=5071$ kcal/m²h, (a) $\alpha_{u\infty}=0.083$, $t_w=15\,\mu$m, (b) $f=1.0$ Hz, $t_w=15\,\mu$m, (c) $\alpha_{u\infty}=0.5$, $f=1.0$ Hz.

the relationship of $\bar{N}_u-\bar{R}_e$ where $\bar{R}_e$ is the Reynolds number based on the time-mean velocity, $\bar{U}_\infty x/\nu$.

The amplitude of wall-temperature oscillation increases rapidly from zero at the leading edge to a saturated value at downstream points (Fig. 3–13). It decreases inversely proportionally to the frequency and increase linearly proportionally to the amplitude of velocity oscillation as seen in Fig. 3–14. Wall-temperature oscillates with a constant phase lag uniformly along the plate (Fig. 3–15). The phase advances from 180°-lag of quasi-steady flow as the frequency of velocity oscillation increases, but it is not influenced by the amplitude (Fig. 3–16). This means that at higher frequencies the convective effect predominates over the thermal inertia effect to transfer heat from the wall to the adjacent fluid.

From the thermal condition of the wall, Eq. (2-7), the amount of oscillating heat flux from the wall to the air flow is balanced by the thermal inertial of the wall plate because its time mean is always equal to the rate of heat released at the wall;

$$-\lambda\left\{\left(\frac{\partial\theta}{\partial y}\right)_{y=0}-\left(\frac{\partial\bar{\theta}}{\partial y}\right)_{y=0}\right\}=\rho_w c_w t_w\frac{\partial\theta_w}{\partial t},\qquad -\lambda\left(\frac{\partial\bar{\theta}}{\partial y}\right)_{y=0}=q$$

(a)

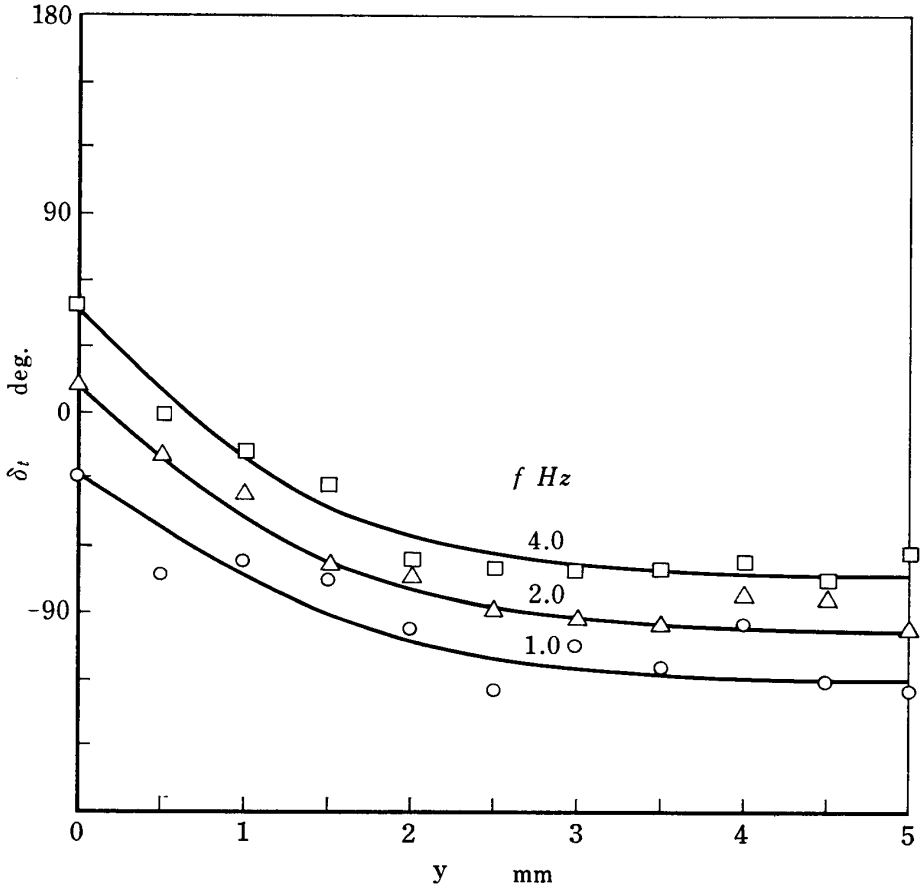

(b)

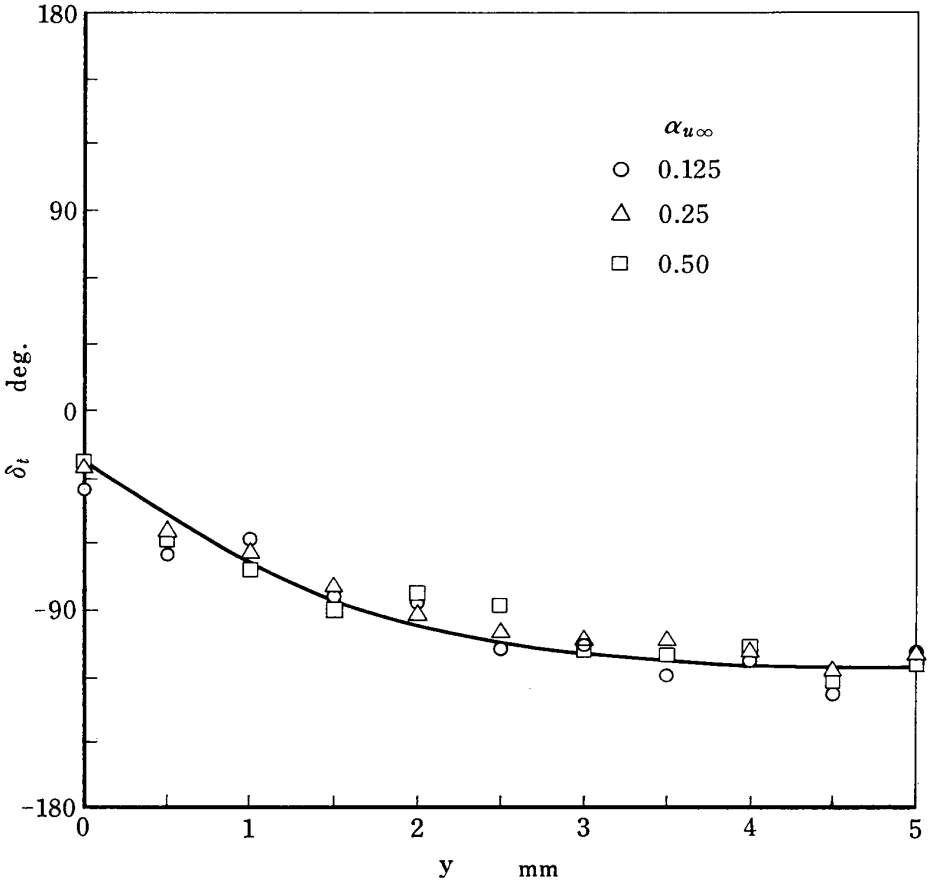

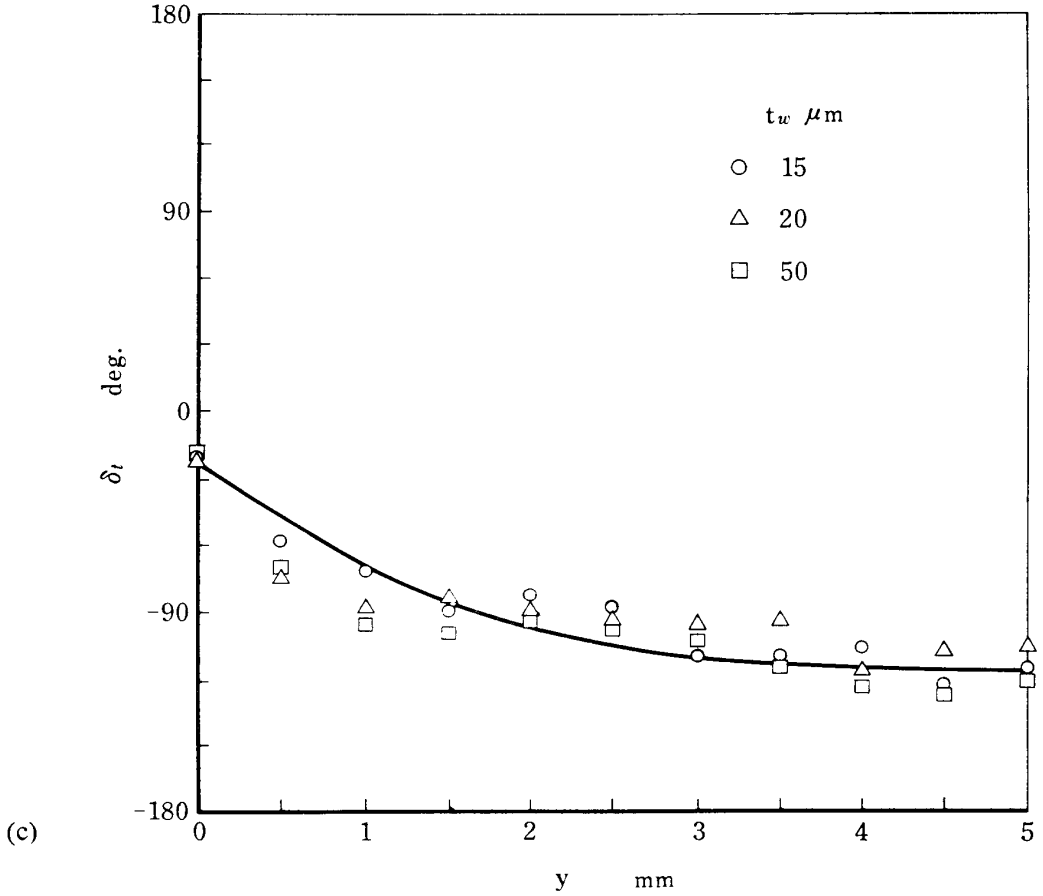

FIG. 3-10. Phase distribution of temperature oscillation in the boundary layer; $\bar{U}_\infty=30$ m/s, $x=143$ mm, $q=5071$ kcal/m²h, (a) $\alpha_{u\infty}=0.083$, $t_w=15\,\mu$m, (b) $f=1.0$ Hz, $t_w=15\,\mu$m, (c) $\alpha_{u\infty}=0.5$, $f=1.0$ Hz.

The oscillating heat flux, that is, the oscillation of heat-transfer rate depends the regenerative behavior of heat capacity of the wall plate. Since in the present case $|\Delta\theta_w/\bar{\theta}_w|\ll 1$ and $\rho_w c_w t_w \omega\bar{\theta}_w/q=\mathrm{O}(1)$, Eq. (2–15) tells that $|\Delta\theta_w/\bar{\theta}_w|$ is proportional to $|\Delta h/\bar{h}|$ or $|\Delta h|$.

4. HEAT TRANSFER FROM A CYLINDER IN OSCILLATING FLOWS

A heated cylinder was located in oscillating air flows, and its wall temperatures were measured to obtain the heat transfer characteristics. The cylinder wall was made of a stainless steel foil of 20 μm or 50 μm thick and 43 mm long which covered a bakelite pipe of 8 mm in diameter as shown in Fig. 4–1. The stainless steel foil was heated electrically by an alternating current. At both sides of the foil, anxiliary electric heaters were employed to avoid the conduction heat loss of the cylinder in the axial direction. The surface temperatures of the foil were measured circumferentially by rotating the cylinder with a copper-constantan thermocouple of 18 μm in diameter soldered to the foil surface.

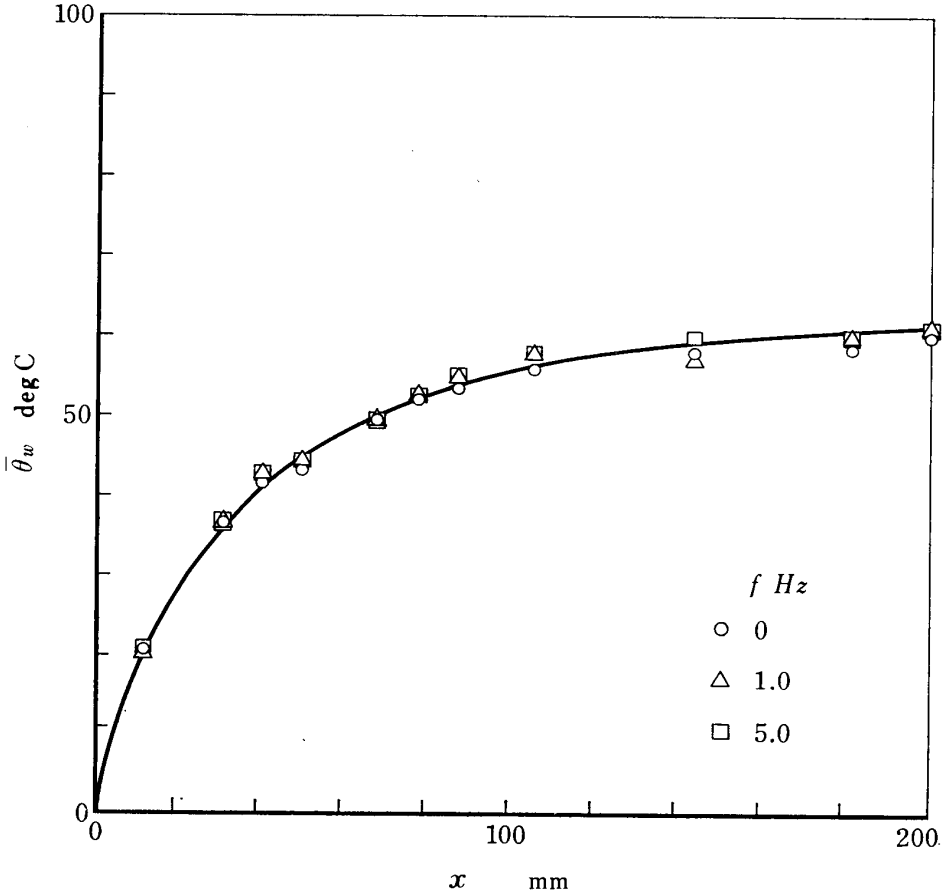

FIG. 3-11. Time-mean wall temperature distribution along the plate; $U_\infty=30$ m/s, $\alpha_{u=}=0.083$, $t_w=15\,\mu$m, $q=5071$ kcal/m²h.

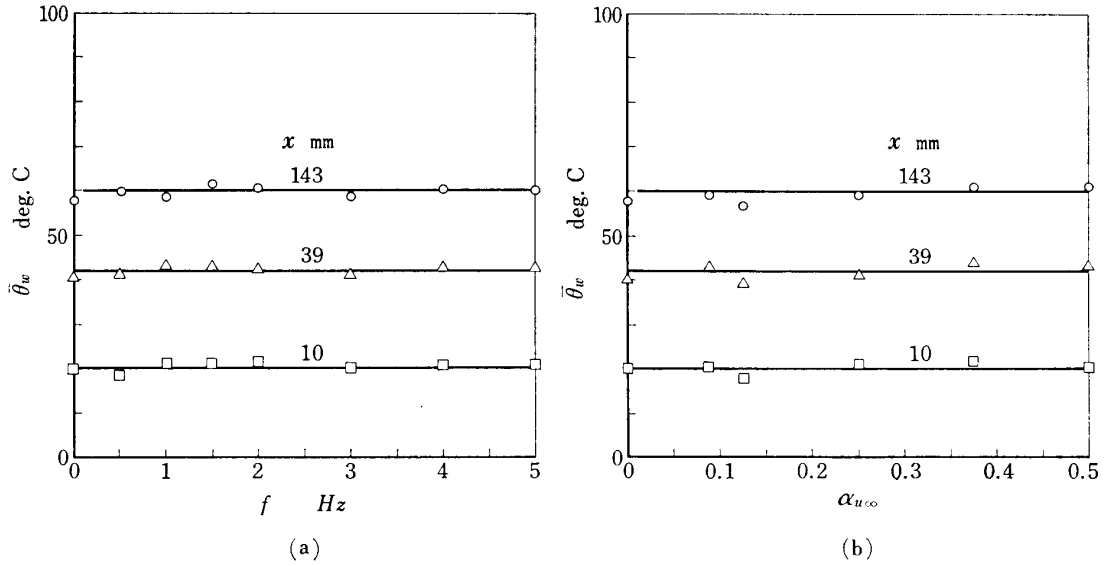

FIG. 3-12. Effect of frequency and amplitude of velocity oscillation on the time-mean wall temperature; $\overline{U}_\infty=30$ m/s, $\alpha_{u\infty}=0.083$(a), $f=1.0$ Hz(b), $t_w=15\,\mu$m, $q=5071$ kcal/m²h.

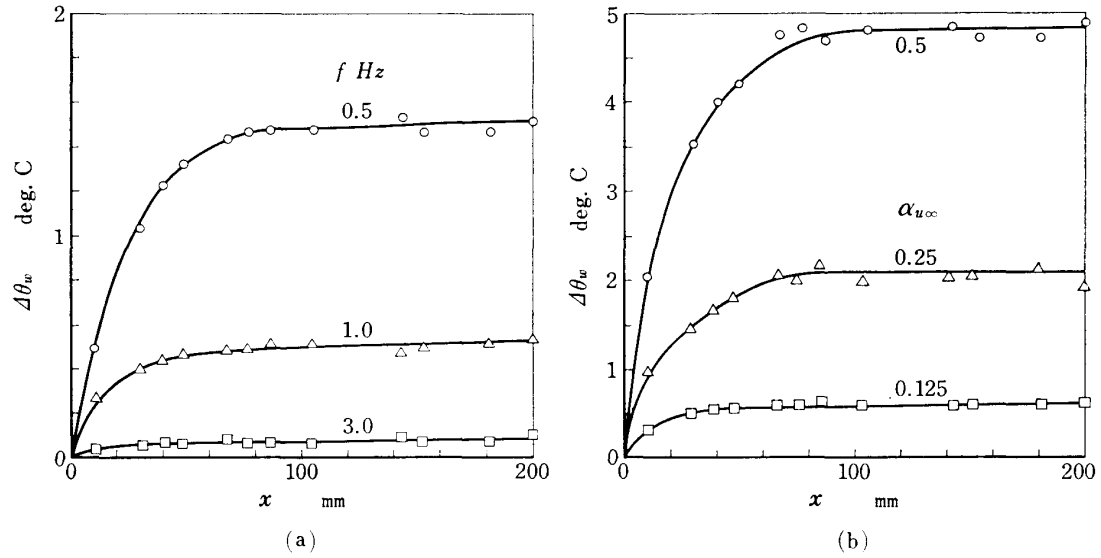

FIG. 3-13. Amplitude distribution of wall-temperature oscillation along the plate; $\overline{U}_\infty=30$ m/s, $\alpha_{u\infty}=0.083$ (a), $f=1.0$ Hz (b), $t_w=15\,\mu$m, $q=5071$ kcal/m²h.

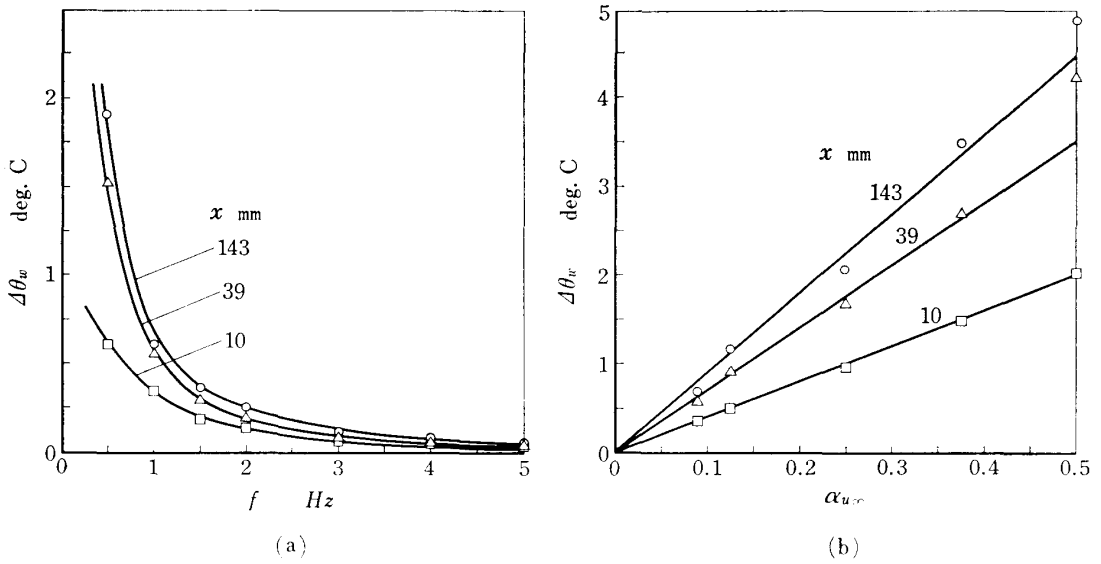

FIG. 3-14. Effect of frequency and amplitude of velocity oscillation on the wall-temperature amplitude; $\overline{U}_\infty=30$ m/s, $\alpha_{u\infty}=0.083$(a), $f=1.0$ Hz(b), $t_w=15\,\mu$m, $q=5071$ kcal/m²h.

4–1 *Wall temperature distribution*

The experimental conditions were varied in the range of

velocity oscillation: $\overline{U}_\infty=10\sim40$ m/s, $\alpha_{u\infty}=0\sim0.5$, $f=0\sim5.0$ Hz,
heat flux: $q=10^3\sim10^5$ kcal/m²h,
heater thickness: $t_w=20,\ 50\,\mu$m,

of which two typical conditions are selected for the following illustration of the results;

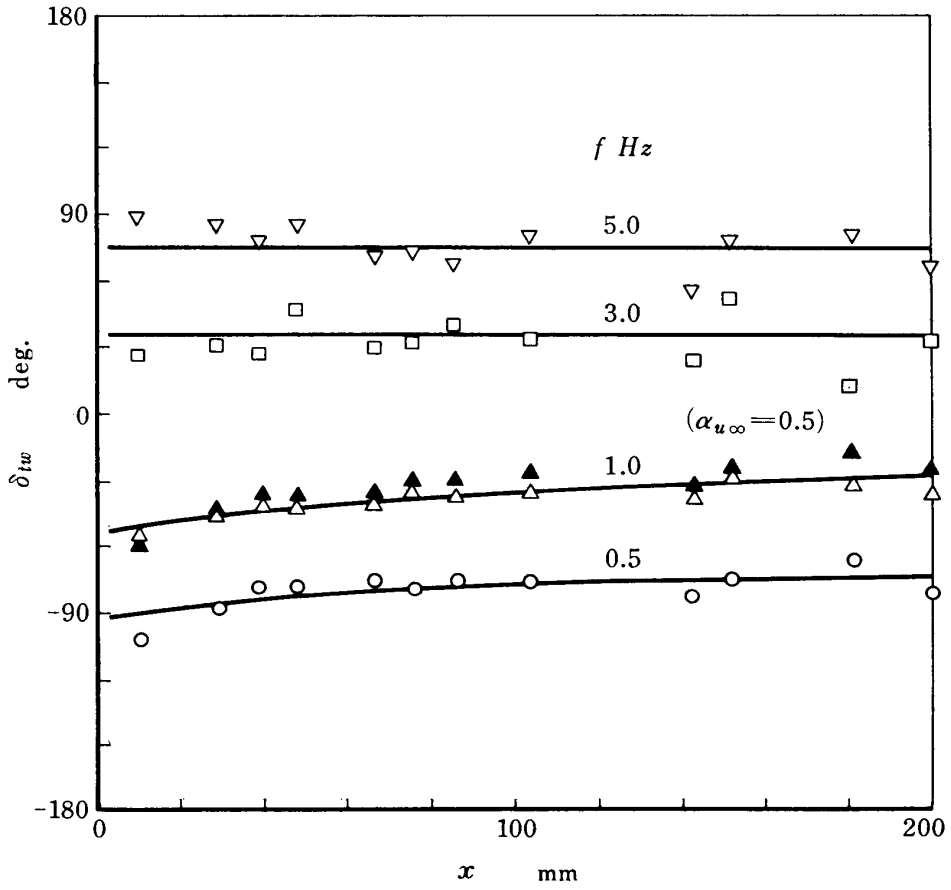

FIG. 3-15. Phase distribution of wall-temperature oscillation along the plate; $\overline{U}_\infty$=30 m/s, $\alpha_{u\infty}$=0.083 (0.5, ▲), t_w=15 μm, q=5071 kcal/m²h.

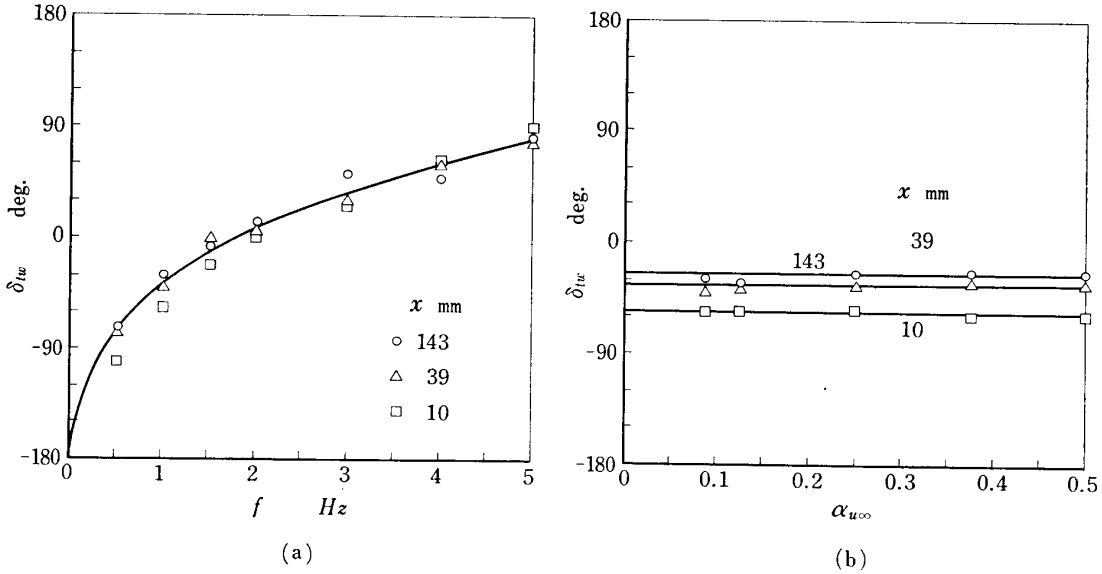

FIG. 3-16. Effect of frequency and amplitude of velocity oscillation on the wall-temperature phase; $\overline{U}_\infty$=30 m/s, $\alpha_{u\infty}$=0.083(a), f=1.0 Hz(b), t_w=15 μm, q=5071 kcal/m²h.

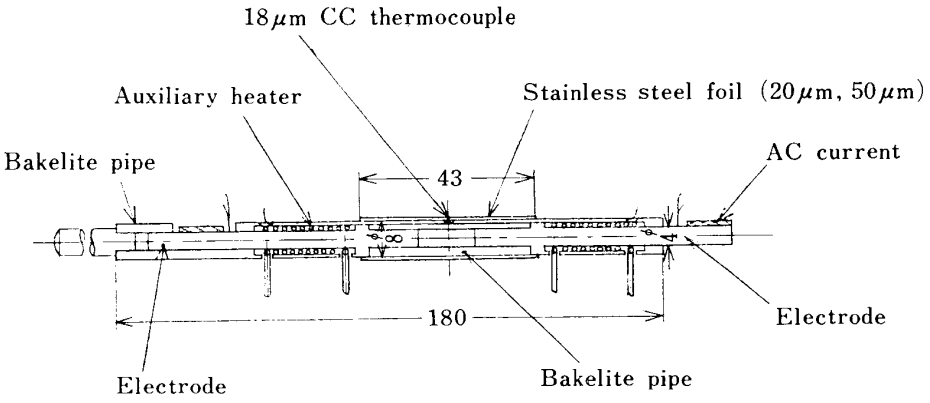

FIG. 4-1. Heated cylinder.

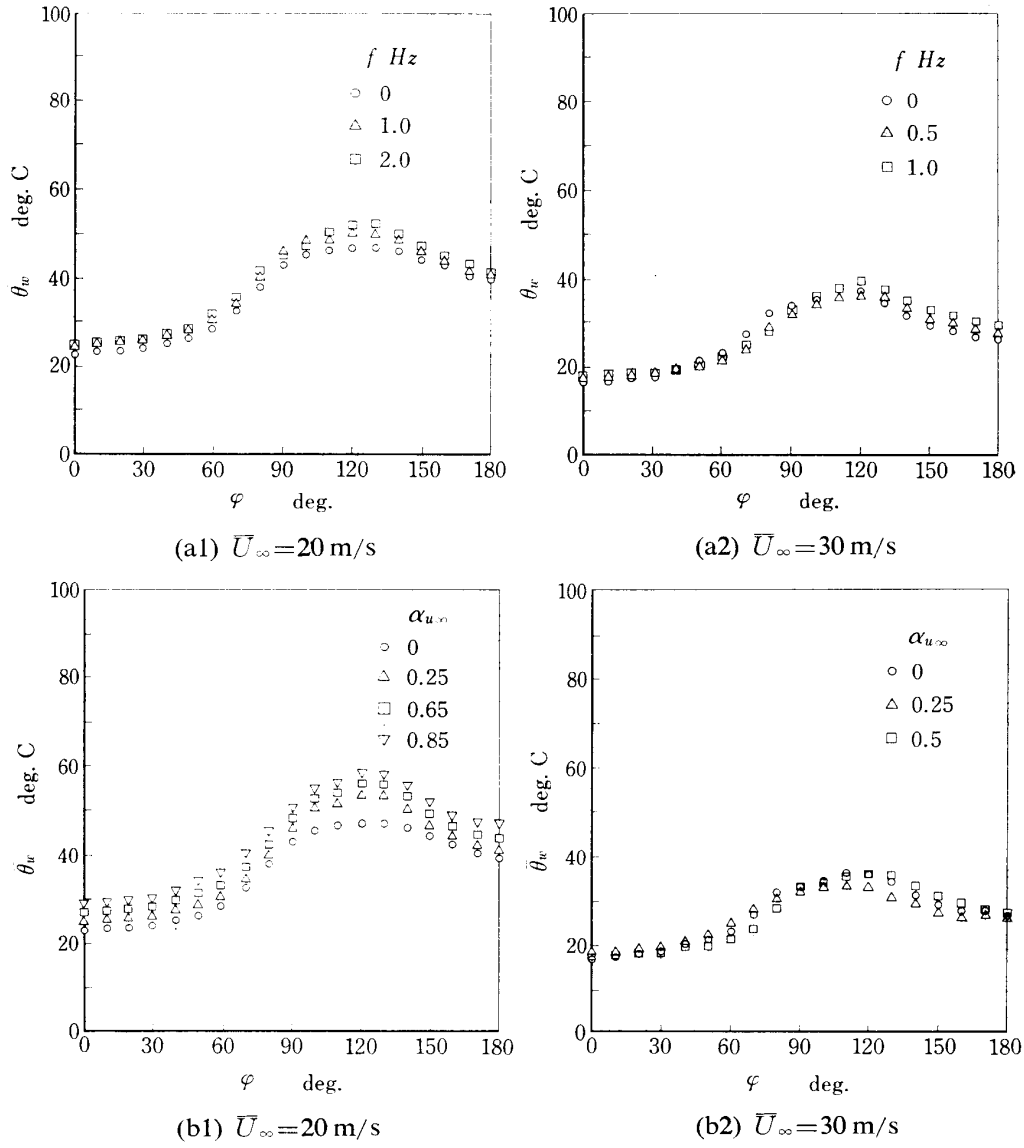

(a1) $\bar{U}_\infty$=20 m/s (a2) $\bar{U}_\infty$=30 m/s

(b1) $\bar{U}_\infty$=20 m/s (b2) $\bar{U}_\infty$=30 m/s

FIG. 4-2. Time-mean wall-temperature distribution around the cylinder; t_w=20 μm, q=5010 kcal/m²h, (1) $\bar{U}_\infty$=20 m/s, $\alpha_{u\infty}$=0.25 (a1), f=1.0 Hz (b1), (2) $\bar{U}_\infty$=30 m/s, $\alpha_{u\infty}$=0.5 (a2), f=1.0 Hz (b2).

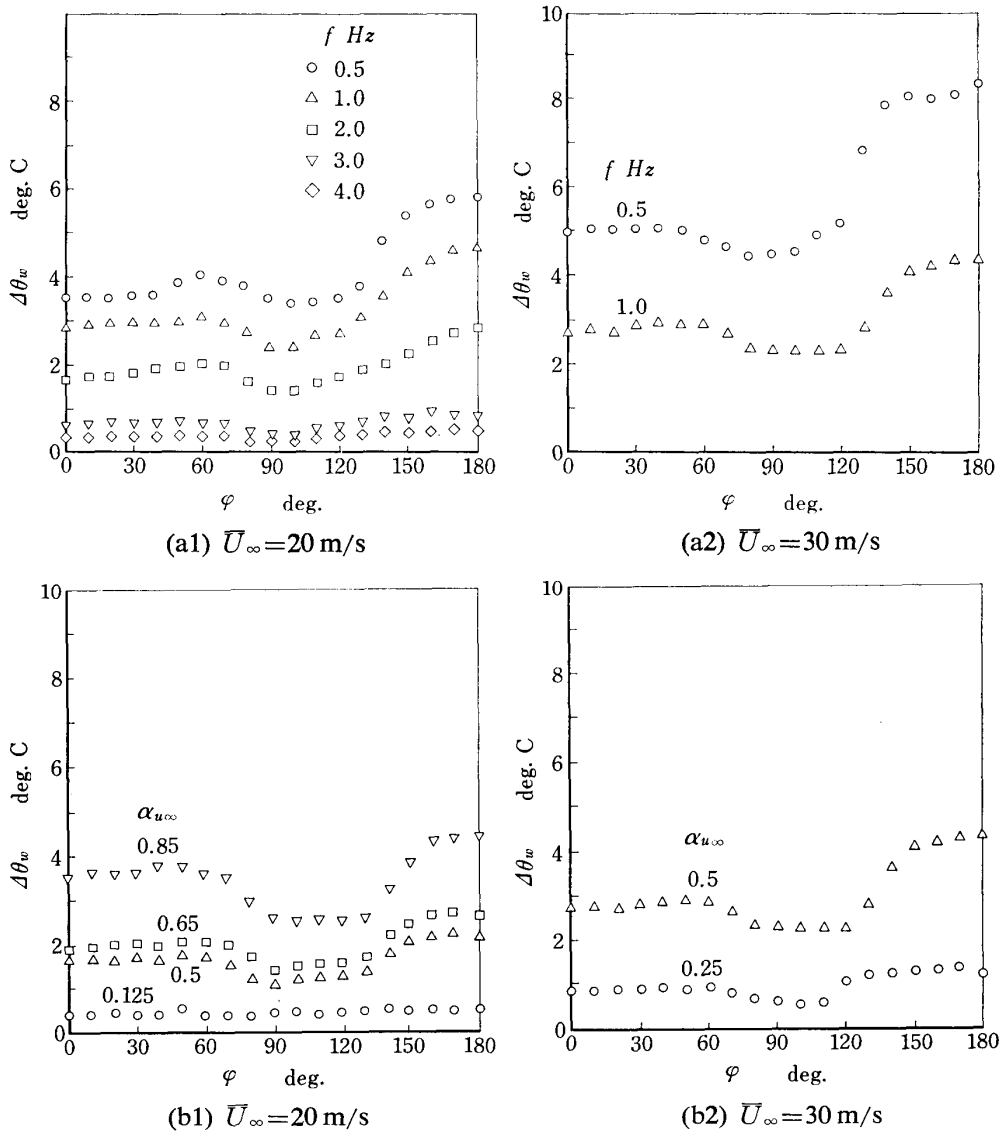

FIG. 4–3. Amplitude distribution of wall-temperature oscillation around the cylinder; t_w=20 μm, q=5010 kcal/m²h, (1) $\overline{U}_\infty$=20 m/s, $\alpha_{u\infty}$=0.25(a1), f=1.0 Hz(b1), (2) $\overline{U}_\infty$=30 m/s, $\alpha_{u\infty}$=0.5(a2), f=1.0 Hz(b2).

(a) $\overline{U}_\infty$=20 m/s, $\alpha_{u\infty}$=0.25, t_w=20 μm, q=5010 kcal/m²h,

(b) $\overline{U}_\infty$=30 m/s, $\alpha_{u\infty}$=0.5, t_w=20 μm, q=5010 kcal/m²h.

The circumferential distributions of time-mean wall temperature are shown in Fig. 4–2 for different frequencies and amplitudes of velocity oscillation. As the frequency and amplitude increase, the time-mean wall temperature increases slightly by the same amount at all circumferential positions. The amplitude of the wall temperature increases with increasing the amplitude of velocity oscillation but decreases with its frequency as shown in Fig. 4–3. It takes a constant value from the foward stagnation to near the separation point ($0<\varphi<60°$), and decreases to take a minimum at the separation point. And then it increases in the separated region ($120<\varphi<180°$). This means that the flow structure in the separated region is highly sensitive to the

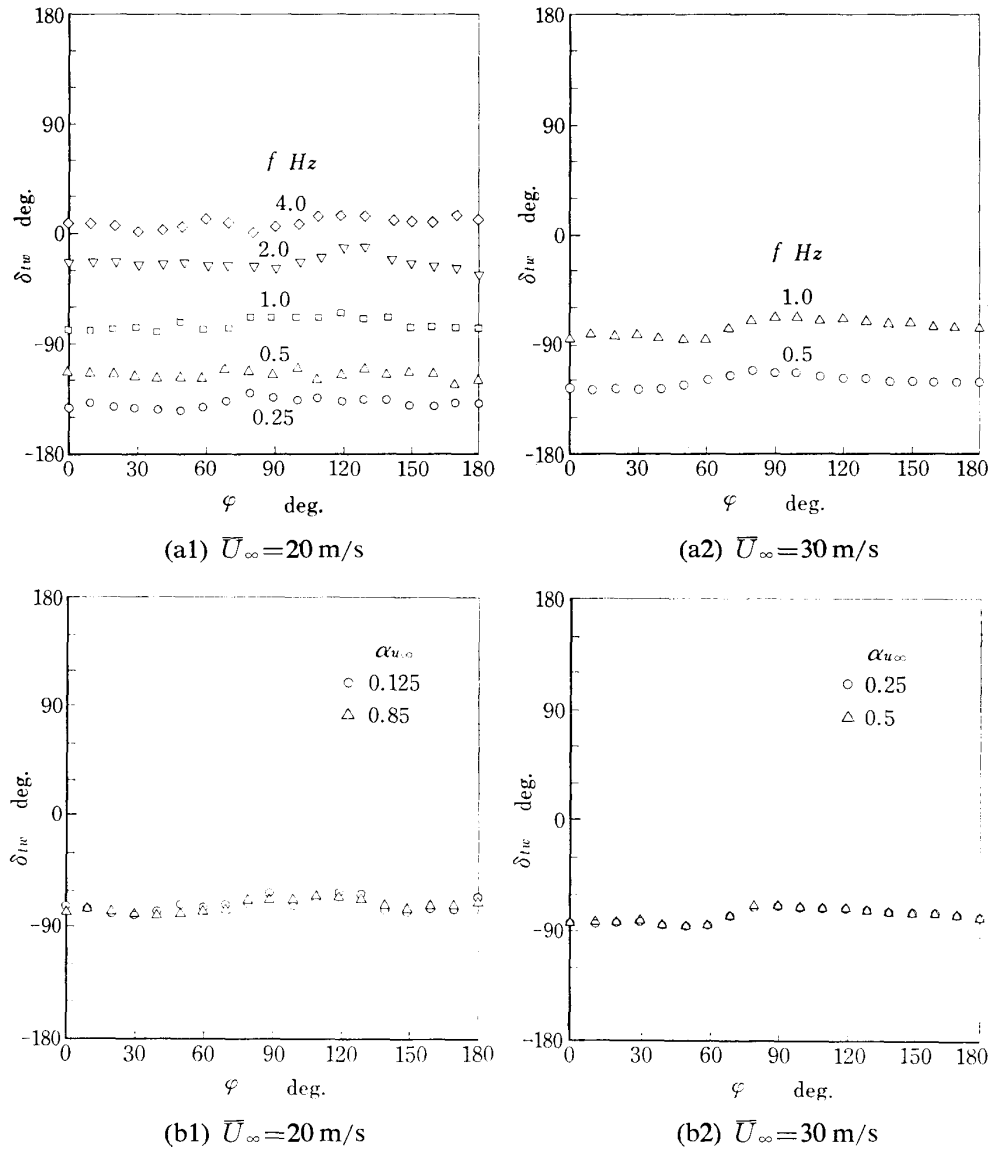

FIG. 4-4. Phase distribution of wall-temperature oscillation around the cylinder; t_w=20 μm, q=5010 kcal/m²h, (1) $\overline{U}_\infty$=20 m/s, $\alpha_{u\infty}$=0.25(a1), f=1.0 Hz(b1), (2) $\overline{U}_\infty$=30 m/s, $\alpha_{u\infty}$=0.5(a2), f=1.0 Hz(b2).

main flow oscillation, whereas the heat convection close to the separation point is less affected by the oscillation. The phase of the wall temperature shown in Fig. 4-4 is hardly influenced by the amplitude of velocity oscillation but at higher frequencies it advances from 180° lag of the quasi-steady flow to an in-phase oscillation with the main flow. It is very interesting that there is little phase difference of the wall temperatures in the circumferential direction in which the flow experiences a considerable change in its structure. The wall temperatures associated with the velocity oscillation oscillate with larger amplitudes and nearly off-phase at lower frequencies, and with smaller amplitudes and nearly in-phase at higher frequencies. These features are similar to those of a flat plate mentioned in the preceeding chapter.

4–2 *Heat transfer characteristics.*

By using the wall temperature, the local heat transfer coefficient is defined as

$$h_\varphi \theta_w = q - \rho_w c_w t_w \frac{\partial \theta_w}{\partial t}.$$

The time-mean local heat transfer coefficient $\bar{h}_\varphi$ is then

$$\bar{h}_\varphi = \frac{q}{\bar{\theta}_w},$$

or in a dimensionless from of the Nusselt number

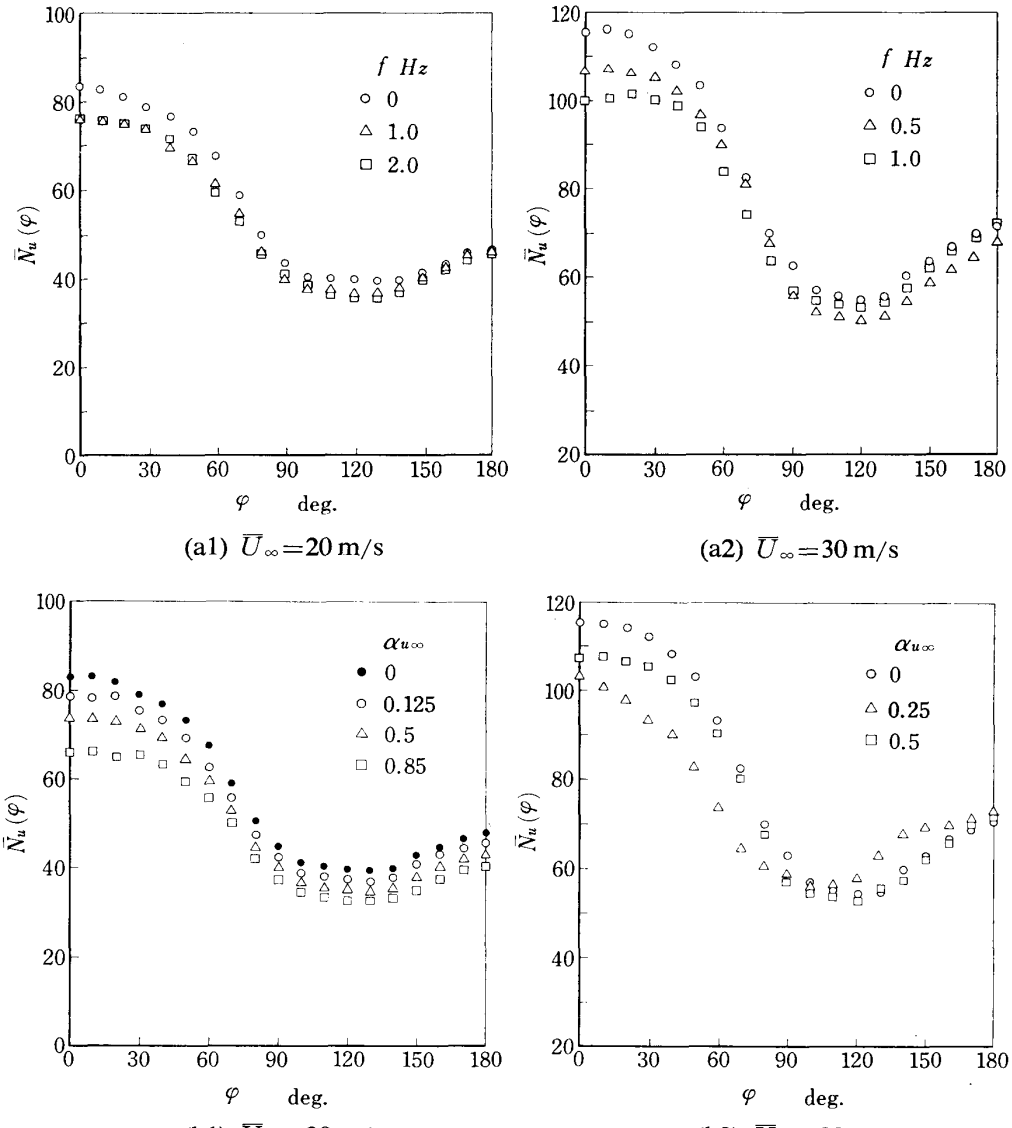

FIG. 4–5. Local Nusselt number; t_w=20 μm, q=5010 kcal/m²h, (1) U_∞=20 m/s, $\alpha_{u\infty}$=0.25(a1), f=1.0 Hz(b1), (2) $\bar{U}_\infty$=30 m/s, $\alpha_{u\infty}$=0.5(a2), f=1.0 Hz(b2).

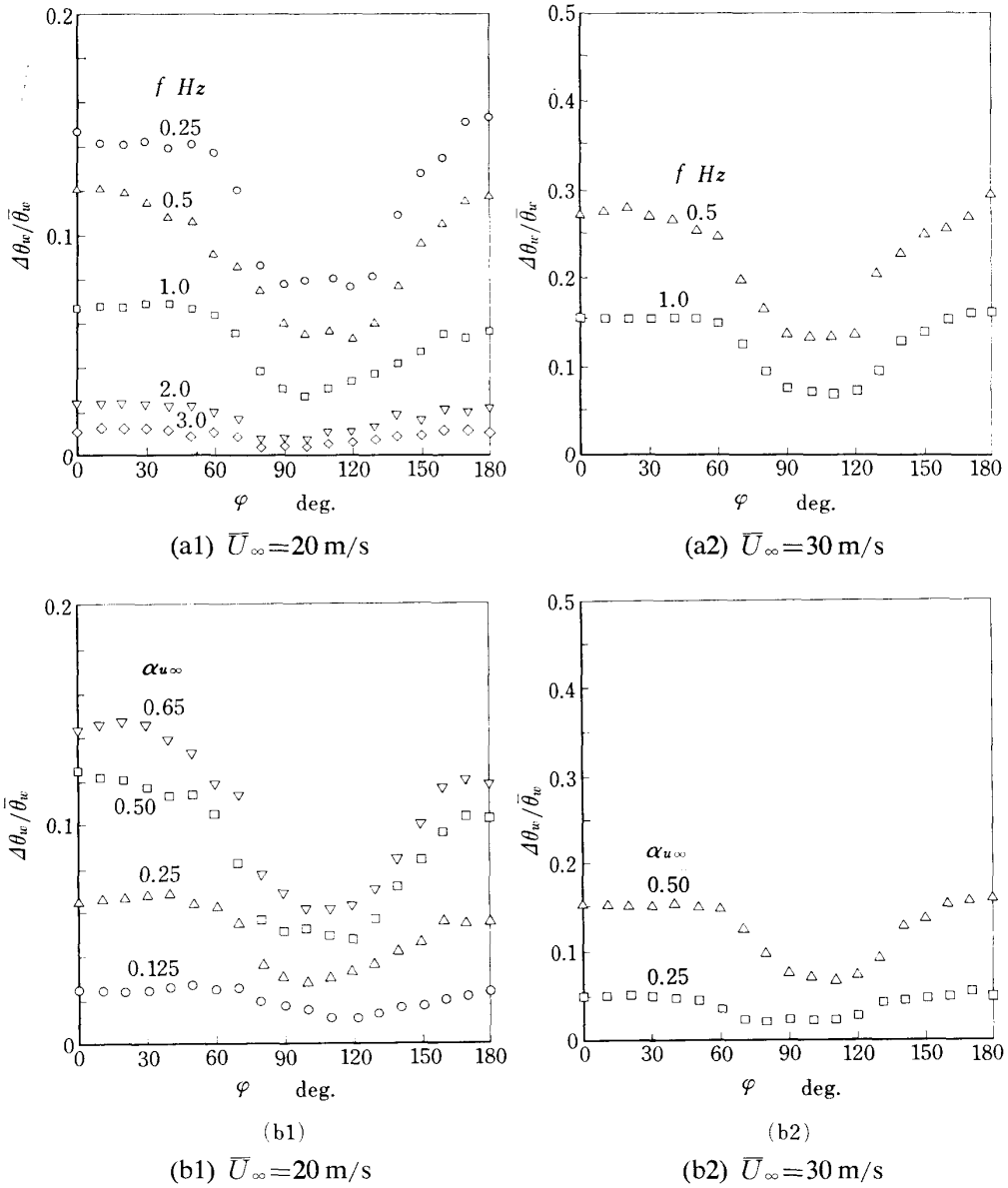

FIG. 4-6. $\Delta\theta_w/\bar{\theta}_w$; t_w=20 μm, q=5010 kcal/m²h, (1) $\bar{U}_\infty$=20 m/s, $\alpha_{u\infty}$=0.25(a1), f=1.0 Hz(b1), (2) $\bar{U}_\infty$=30 m/s, $\alpha_{u\infty}$=0.5(a2), f=1.0 Hz(b2).

$$\bar{N}_u(\varphi)=\frac{\bar{h}_\varphi d}{\lambda}.$$

The distributions of local time-mean Nusselt number are shown in Fig. 4–5. It tends to deteriorate at higher frequencies and larger amplitudes of velocity oscillation, especially in the region close to the forward stagnation point. In order to show the amplitudes of the local heat transfer coefficient, $|\Delta h(t)|$, the values of $\Delta\theta_w/\bar{\theta}_w$ are shown in Fig. 4–6. They are affected considerably by the frequency and amplitude of main flow oscillation especially in the forward region close to the stagnation point and in the separated region.

The overall heat transfer coefficient $\bar{h}_m$ can be defined as

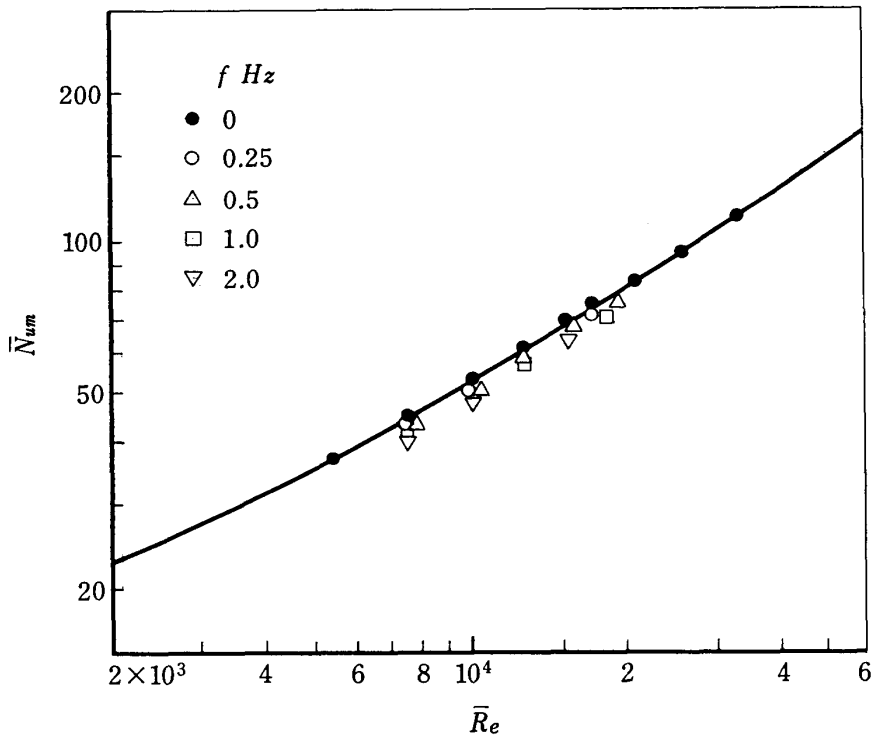

FIG. 4–7. Overall Nusselt number vs. Reynolds number; $\bar{U}_\infty=20\sim40$ m/s, $\alpha_{u\infty}=0\sim0.5$, $t_w=15, 20, 50\mu$m.

$$\bar{h}_m=\frac{q}{\frac{1}{\pi}\int_\pi^0 \bar{\theta}_w(\varphi)d\varphi}$$

of which a dimensionless form $\bar{N}_{um}=\bar{h}_m d/\lambda$ is the overall Nusselt number. The latter is shown in Fig. 4–7 with respect to the time-mean Reynolds number $\bar{R}_e(=\bar{U}_\infty d/\nu)$. It keeps the relation for steady flows (solid line), in the form of

$$\bar{N}_{um}=c\bar{R}_e^n$$

of which the proportional constant c varies with the main flow oscillation, taking slightly smaller values as increasing the frequency and amplitude. It is seen from the figure that the overall Nusselt numbers are reduced slightly with the main flow oscillation.

5 HEAT TRANSFER FROM A CYLINDER-ABOVE-PLATE SYSTEM IN OSCILLATING FLOWS

A heated cylinder is located above a flat plate parallel to the main-flow. By changing the distance between the cylinder and the plate, the temperature distribution in the boundary layer of the plate and the wall temperatures of the cylinder and the plate were measured to obtain the heat transfer characteristics of the system. The geometrical configuration and the coordinates are illustrated in Fig. 5–1. The

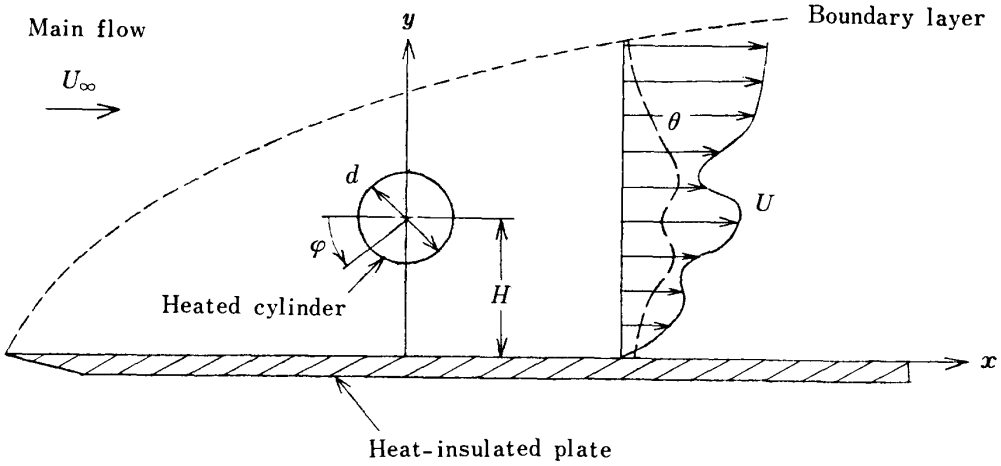

FIG. 5-1. Configuration of a heated cylinder above a flat plate.

x-coordinate is measured from the center of the cylinder along the plate and the y-coordinate is perpendicular to the plate surface. The distance between the plate surface to the center of the cylinder is denoted by H, and the azimuth from the cylinder center by φ. The flat plate was a plain bakelite plat of 2 mm thick, 59 mm wide and 200 mm long. The heated cylinder was located at the point of about 100 mm from the leading edge and $H=2\sim20$ mm above the plate surface where the boundary layer of velocity had a thickness of $6\sim7$ mm at $\overline{U}_\infty=20\sim30$ m/s. The heated cylinder was made of a thin stainless steel foil of 15, 50, 100, 300 μm in thickness covered a bakelite cylinder. The diameter of the cylinder was 3.2, 5.2 and 10.3 mm which correspond approximately to 1/2, 1 and 2$\times$(thickness of the boundary layer), respectively. The length of the heater section was 40 mm long, having an auxiliary heater of 5 mm long at both sides to prevent heat loss from the main heater by conduction.

The surface temperatures of the heater were measured with a 18 μm thermocouple of copper-constantan soldered to the foil. For the measurement of temperatures of air flow in the boundary layer, a 18 μm thermocouple of copper-constantan was also used. The experimental conditions were in the range of velocity oscillation; $\overline{U}_\infty=10\sim40$ m/s, $\alpha_{u\infty}=0\sim0.5$, $f=0\sim5$ Hz.

5-1 *Heat transfer from a cylinder above a flat plate*

Surface temperature distribution

In Fig. 5-2, the surface temperature distribution of the heated cylinder located in oscillating main flows is shown for different distances H. It is not symmetric with respect to $\varphi=0°$ due to the effect of the plate. As the distances H becomes smaller, the asymmetry becomes more appreciable in the way that the surface faced to the plate takes lower temperatures than the opposite surface does. In addition, the separation point moves more rearward and the surface temperatures become higher in the separated region. The surface temperatures are ,however, hardly affected by the frequency and amplitude of velocity oscillation.

The amplitudes of surface temperature are shown in Fig. 5-3, being considerably

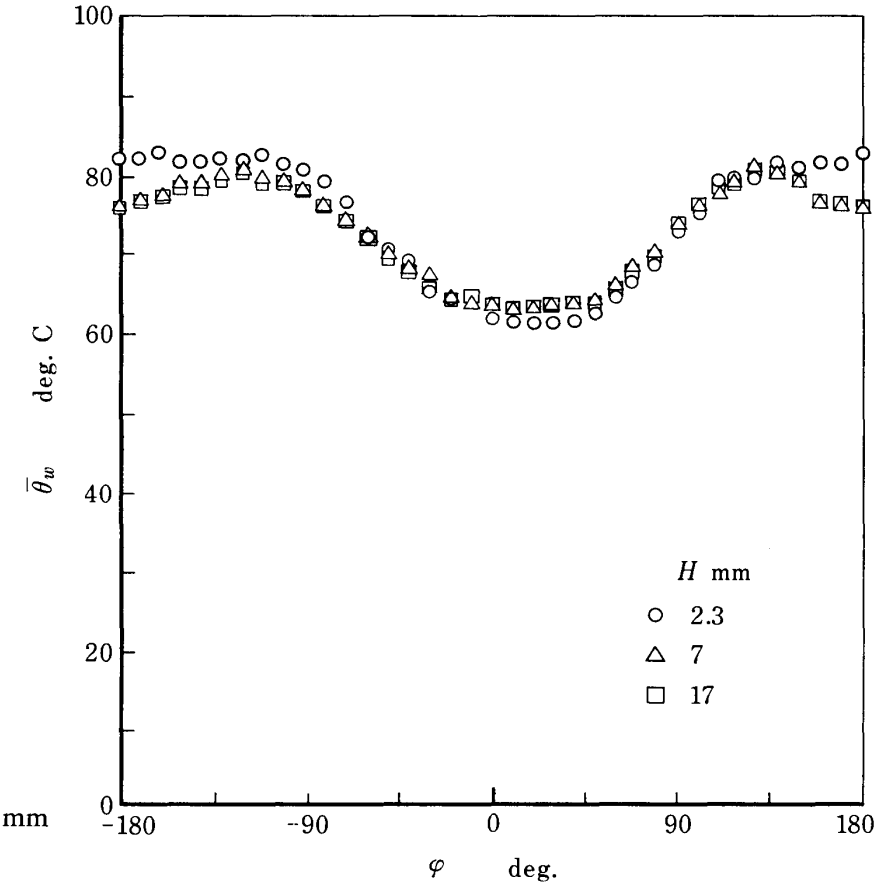

(a) d=3.2 mm

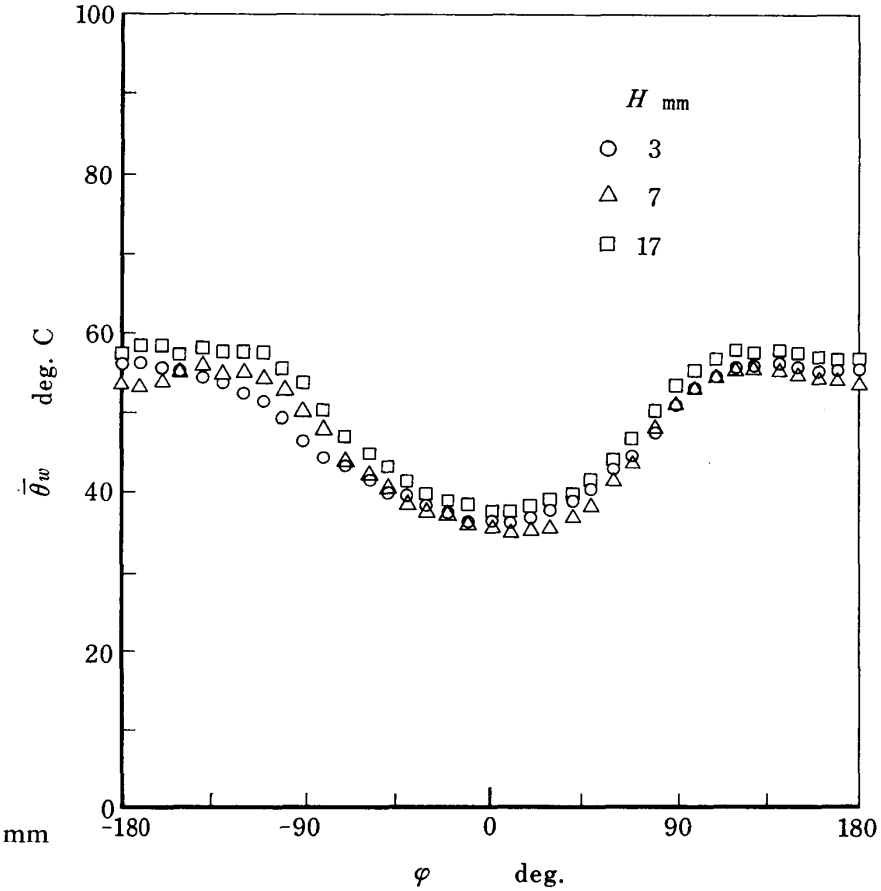

(b) d=5.2 mm

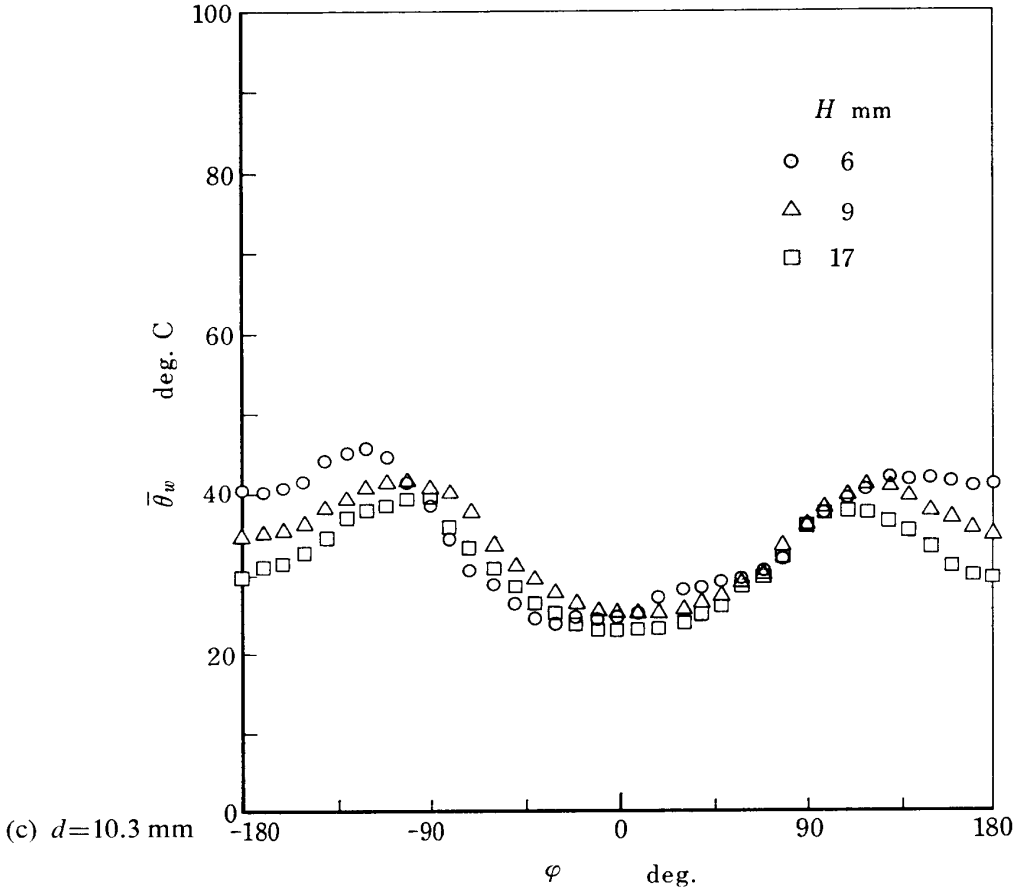

FIG. 5–2. Time-mean wall-temperature distribution around the cylinder; $\bar{U}_\infty =$ 30 m/s, $\alpha_{u\infty}=0.33$, $f=1.0$ Hz, $t_w=100\,\mu$m, $Q=9.28$ kcal/h, $d=3.2$ mm(a), 5.2 mm(b), 10.3 mm(c).

affected by the frequency and amplitude of velocity oscillation. The surface temperature has larger amplitude at lower frequencies and larger amplitudes of velocity oscillation. Close to the separation point, they affect less efficiently to result in a minimum of the circumferential distribution. These effects are same as those for the case of a cylinder in oscillating flow without the plate. The asymmetry of amplitude distribution arises only through the change in the separation point.

The phase relation is shown in Fig. 5–4. The surface temperature is almost uniform in phase throughout the wall surface. Its phase is affected considerably by the frequency of velocity oscillation but hardly by the amplitude. With increasing the frequency, the phase advances from $\delta_{tw}=-180°$ to $\delta_{tw}=0°$. The effects of the frequency and amplitude of velocity oscillation are also same as those for a single cylinder. The plate make little change in phase difference of the wall temperature.

Heat transfer coefficients

Figure 5–5 shows the relationship between the overall time-mean heat transfer coefficient in a dimensionless form, $\bar{N}_{um}$, and the Reynolds number, $\bar{R}_e$. The Nusselt number takes slightly larger values than that of a cylinder without the plate, but is hardly affected by the frequency and amplitude of velocity oscillation within the present experimental conditions.

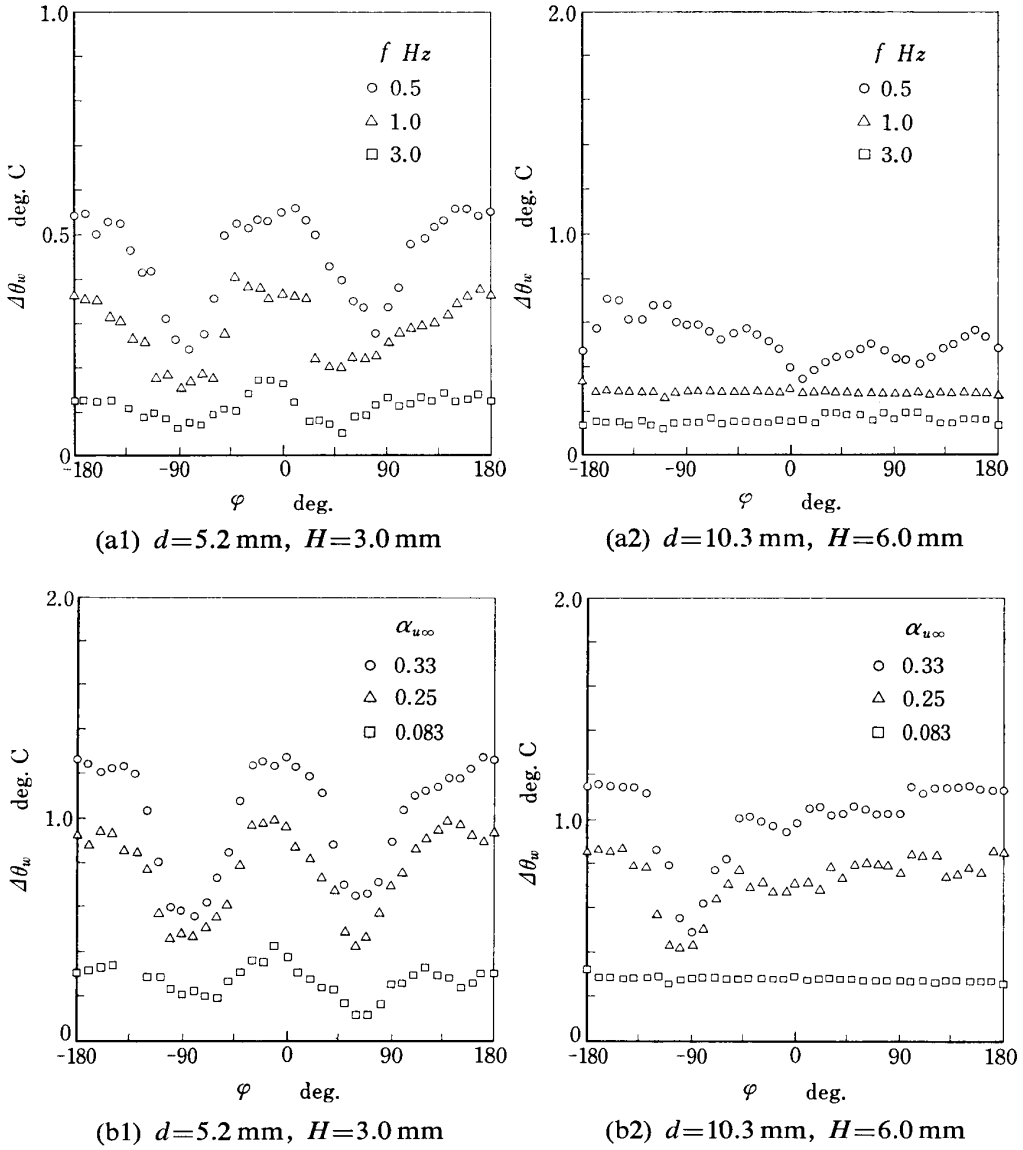

FIG. 5-3. Amplitude distribution of wall-temperature oscillation around the cylinder; $\bar{U}_\infty=30$ m/s, $\alpha_{u\infty}=0.33$ (a), $f=1.0$ Hz (b), $t_w=100\,\mu$m, $Q=9.28$ kcal/h.

Since the phase of oscillating wall-temperatures has little variation throughout the surface, the wall temperatures can be averaged over the surface, being written in the form of

$$\theta_{wm}=\bar{\theta}_{wm}+\frac{\Delta\theta_{wm}}{2}\sin(\omega t+\delta_{twm})$$

where $\delta_{twm}\simeq\delta_{tw}$.

The amplitude of the heat transfer coefficient $\Delta h(t)$ or $\Delta h(t)/\bar{h}$, is given by Eq. (2-15), being proportional to $\Delta\theta_w/\bar{\theta}_w$. The values of $\Delta\theta_w/\bar{\theta}_w$ are illustrated in the following figures to show the effect of the mean velocity, amplitude, frequency, distance and cylinder diameter on the overall heat transfer oscillation. The amplitude and

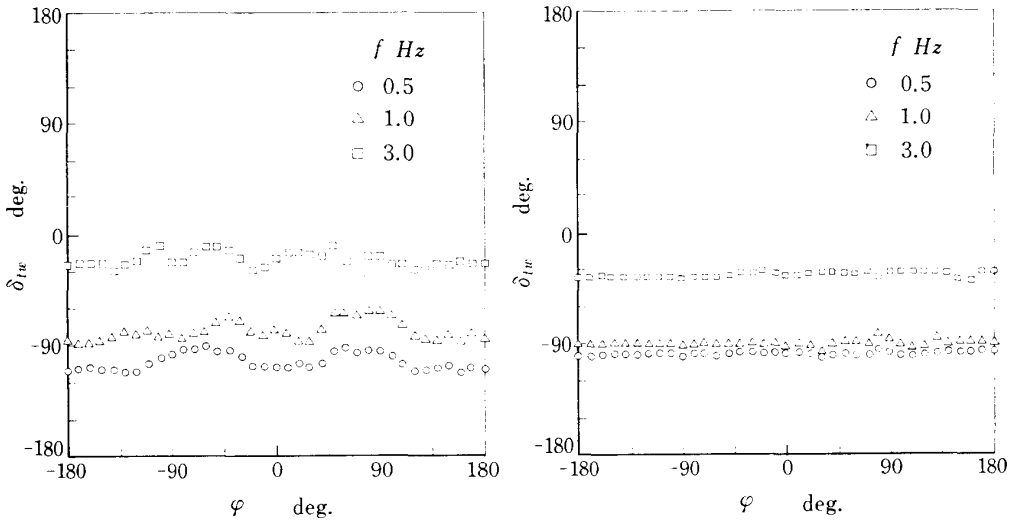

(a1) d=5.2 mm, H=3.0 mm (a2) d=10.3 mm, H=6.0 mm

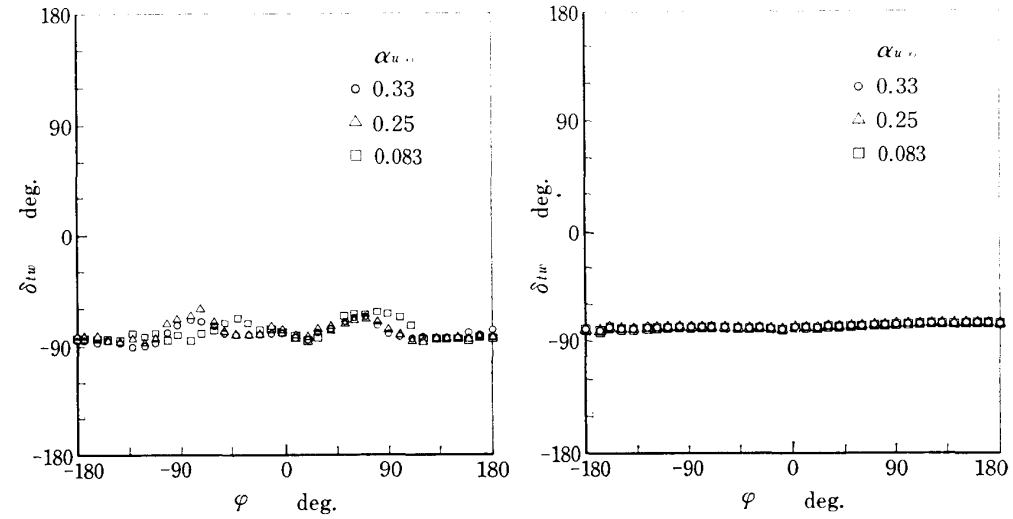

(b1) d=5.2 mm, H=3.0 mm (b2) d=10.0 mm, H=6.0 mm

FIG. 5–4. Phase distribution of wall-temperature oscillation around the cylinder; $\bar{U}_\infty$=30 m/s, $\alpha_{u\infty}$=0.33 (a), f=1.0 Hz (b), t_w=100 μm, Q=9.28 kcal/h.

phase of $\Delta\theta_w/\bar{\theta}_w$ are denoted by α_{hm} and $\delta_{hm}(=\delta_{twm})$, respectively. The value of α_{hm} increases linearly with the mean velocity and the amplitude of the main flow, whereas they have no effect on the phase difference as shown in Figs, 5–6 and 5–7. The frequency of velocity oscillation decreases α_{hm} and increases the phase difference as seen in Fig. 5–8. It is very interesting that the distances between the cylinder and the plate, H, has no effect on both the amplitude and phase as shown in Fig. 5–9. This means that the presence of a plate close to a cylinder has little effect on the amplitude of heat transfer oscillation averaged over the cylinder surface. The diameter of the cylinder has little effect on the amplitude and phase angle as shown in Fig. 5–10. From Fig. 5–11, it is seen that the thickness of the heater foil reduces the amplitude greatly as it increases.

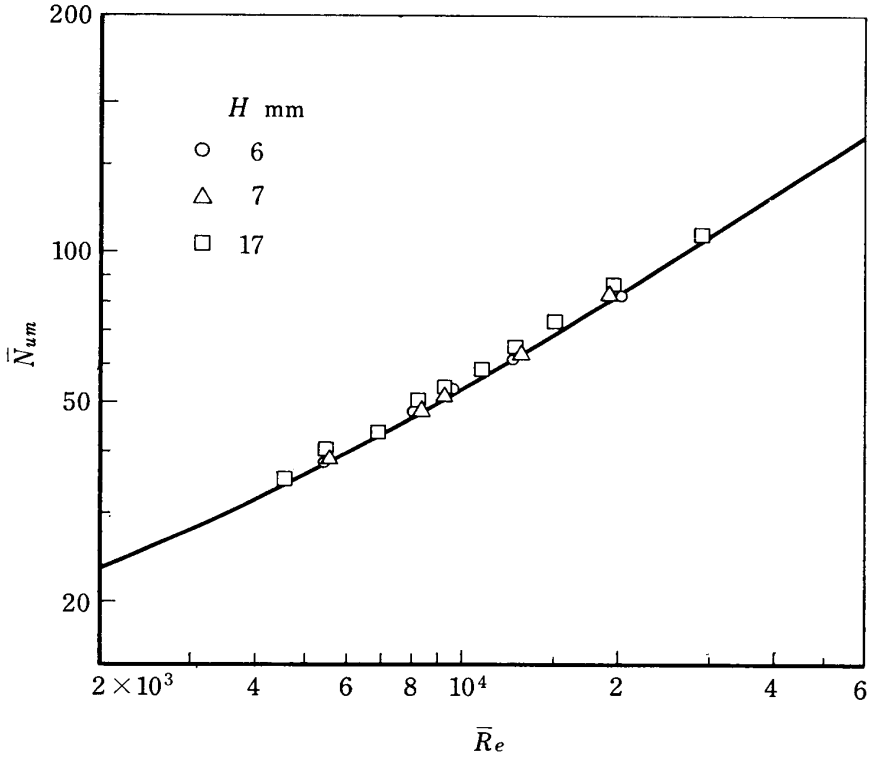

FIG. 5-5. Overall Nusselt number vs. Reynolds number; $\bar{U}_\infty$=20~40 m/s, $\alpha_{u\infty}$=0.33, f=1.0 Hz, d=3.2, 5.2, 10.3 mm.

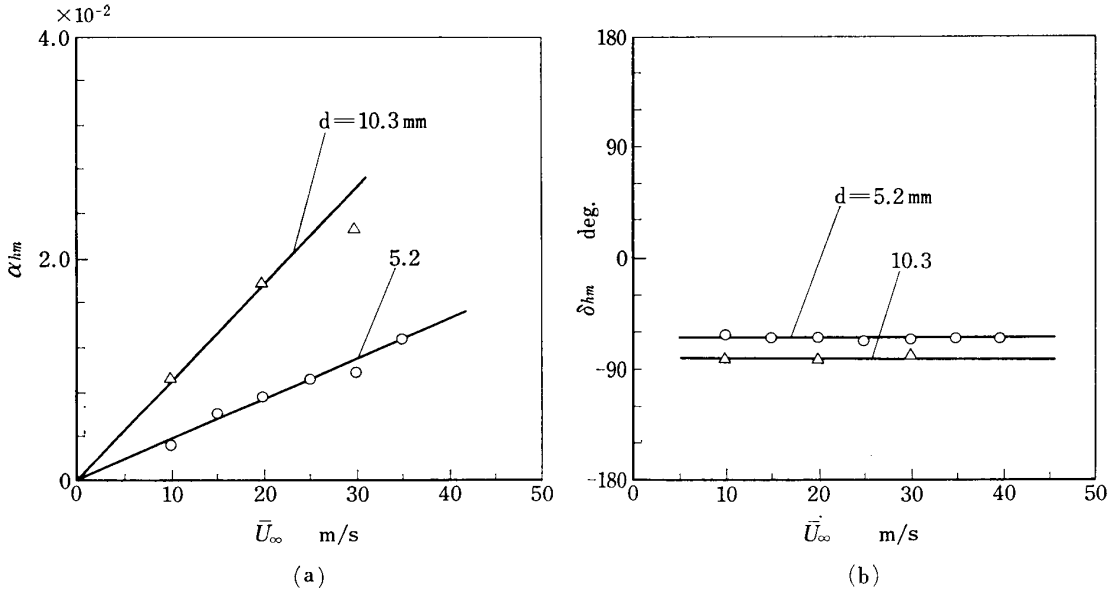

FIG. 5-6. Effect of time-mean velocity on heat transfer oscillation; $\alpha_{u\infty}$=0.25, f=1.0 Hz, H=7.0 mm, t_w=100 μm, Q=9.28 kcal/h.

5-2 *Velocity and temperature distributions in the boundary layer of a cylinder-above-plate system*

Velocity and temperature distributions in the boundary layer of a cylinder-above-plate system located in oscillating flows were measured to investigate the oscillating

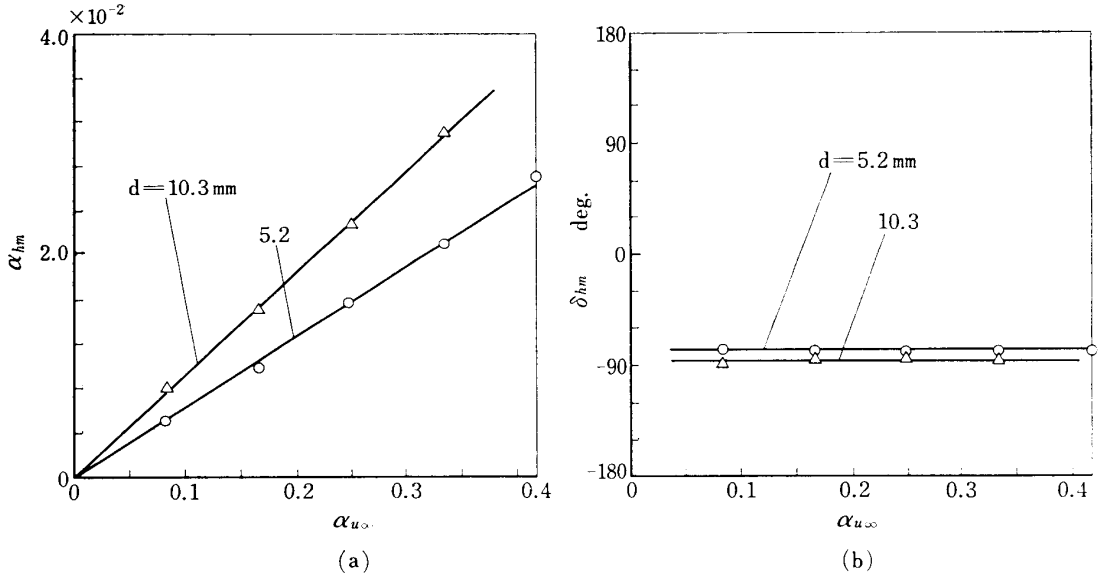

FIG. 5-7. Effect of velocity amplitude on heal transfer oscillation; $\overline{U}_\infty=30$ m/s, $f=$ 1.0 Hz, $H=7.0$ mm, $t_w=100\,\mu$m, $Q=9.28$ kcal/h.

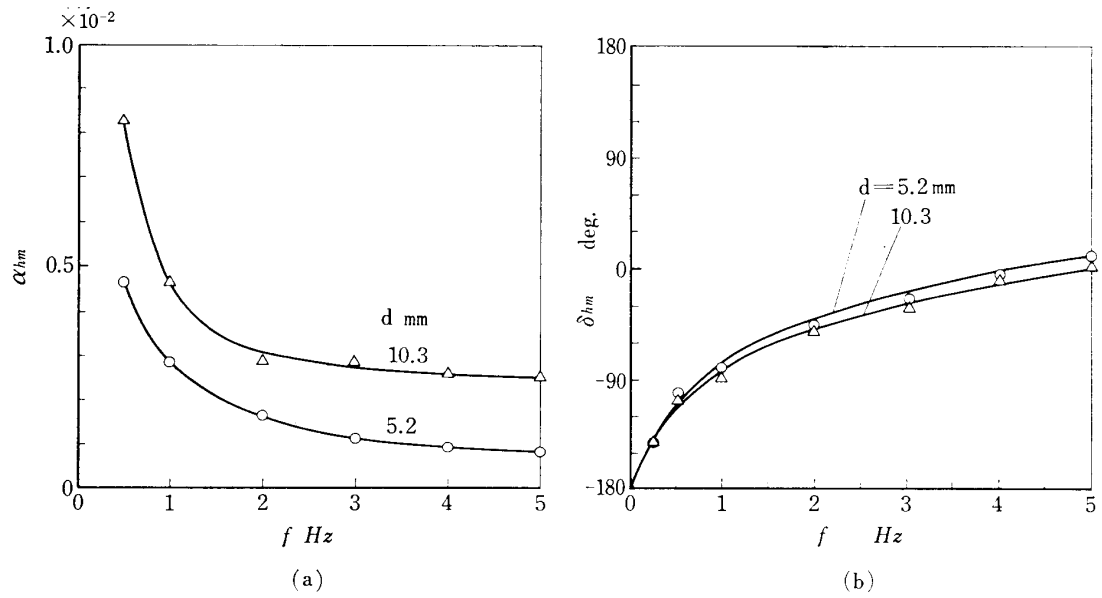

FIG. 5-8. Effect of velocity frequency on heat transfer oscillation $\overline{U}_\infty=30$ m/s, $\alpha_{u\infty}=$ 0.083, $H=7.0$ mm, $t_w=100\,\mu$m, $Q=9.28$ kcal/h.

temperature field behind a heated cylinder close to a flat plate. Since the velocity field should not be altered by the heat addition to the cylinder, it may be evaluated from the measurement of the isothermal field with a hot-wire anemometer. The distributions of time-mean, amplitude and phase diefference of velocity oscillations in the boundary layer behind the unheated cylinder were measured by varying the distance between the cylinder and the plate. The temperature field behind the heated cylinder was investigated with a copper-constantan thermocouple of 18 μm in diameter. The used cylinder and plate were the same ones in the preceding chapters.

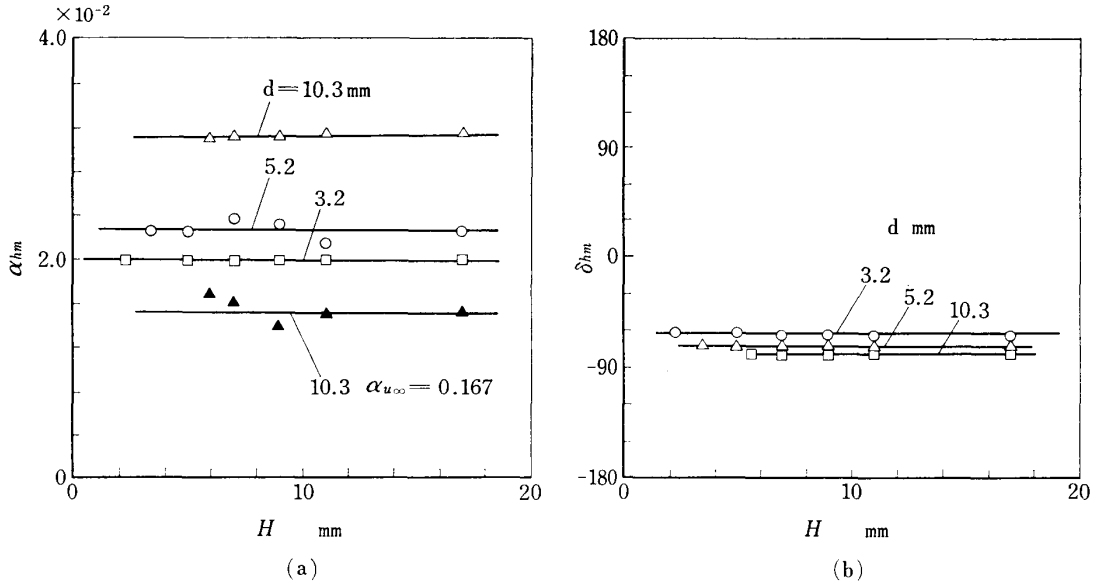

FIG. 5-9. Effect of cylinder location on heat transfer oscillation; $\overline{U}_\infty$=30 m/s, $\alpha_{u\infty}$= 0.33, f=1.0 Hz, t_w=100 μm, Q=9.28 kcal/h.

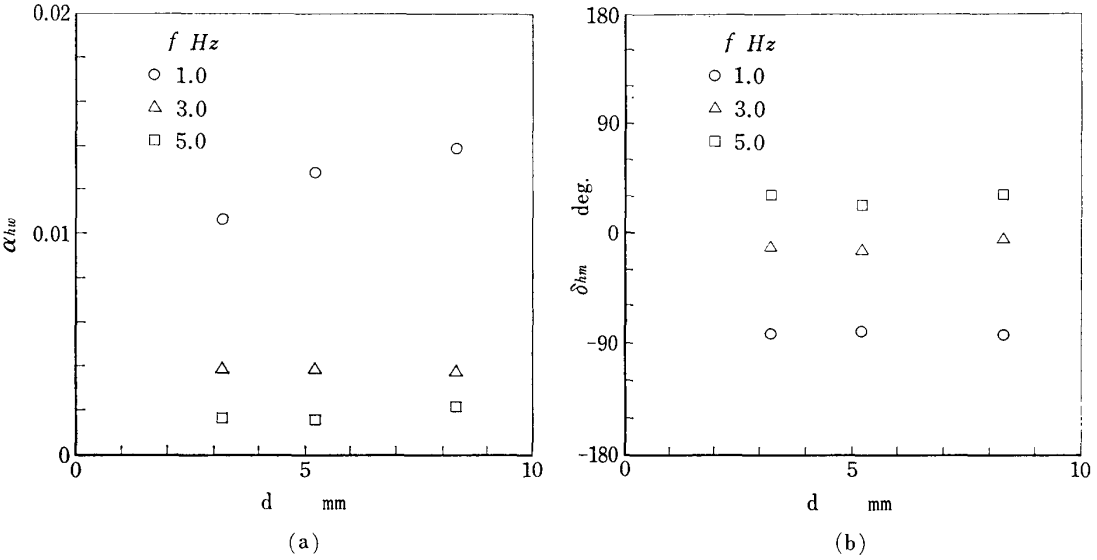

FIG. 5-10. Effect of cylinder diameter on heat transfer oscillation; $\overline{U}_\infty$=30 m/s, $\alpha_{u\infty}$= 0.083, f=1.0 Hz, H=7.0 mm, t_w=15 μm, q=7400 kcal/m²h.

Velocity distributions

Figure 5-12 shows the velocity distribution normal to the plate behind the cylinder at different frequencies of velocity oscillation. The values of H illustrated in the figure correspond to the locations of the cylinder; just outside the boundary layer (H=11.8 mm), in the outer layer (H=6.8 mm) and close to the inner layer (H=3.8 mm). In the case of H=11.8 mm, the velocity distribution close to the plate coincides with the one without the cylinder. A cylinder located close to the inner part of the boundary layer makes the flow to be of double layers. As the distance between the cylinder and the plate increases, the velocity in the region faced to the

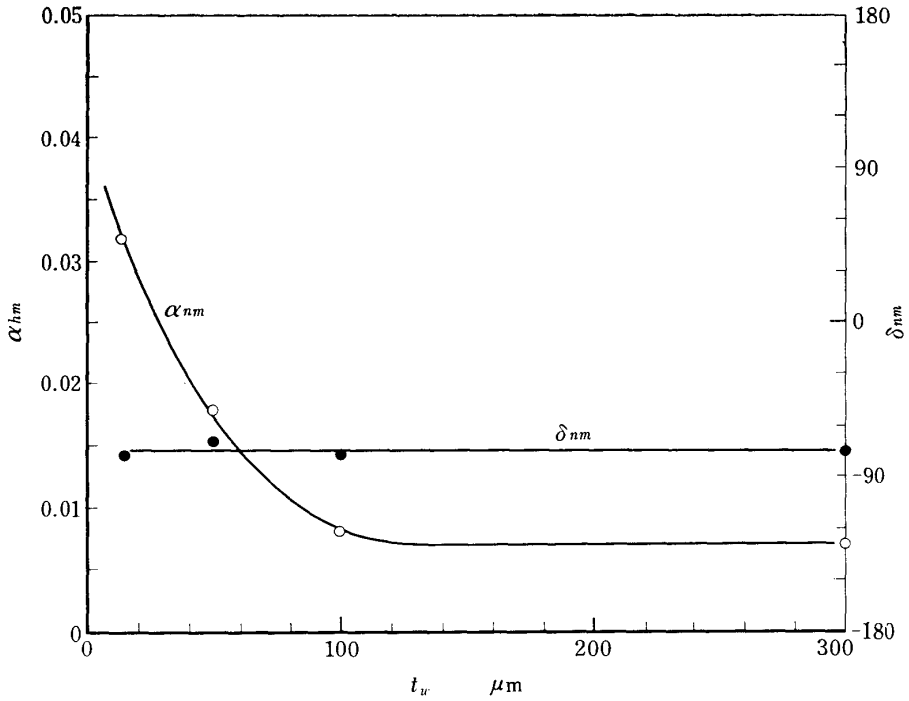

FIG. 5–11. Effect of heater thickness on heat transfer oscillation; $\bar{U}_\infty=30$ m/s, $\alpha_{u\infty}=0.25$, $f=1.0$ Hz, $d=5.0$ mm, $H=7.0$ mm, $q=14530$ kcal/m²h.

cylinder rapidly increases to that of the single boundary layer without the cylinder. Oscillating main flows tend to make the wake flow of the cylinder incline toward the outer layer.

The amplitude distribution shown in Fig. 5–13 is approximately proportional to the time-mean velocity just behind the cylinder, but takes rather more flattened profiles. As far as the phase is concernned, the flow in the boundary layer behind the cylinder follows exactly the main flow.

Temperature distributions

The time-mean temperature close to the cylinder, as shown in Fig. 5–14, is distributed in a similar way of wake flow in a free stream but at further downstream is more diffused at an almost same speed toward the inner and outer layers to become a symmetrical profile. These interesting features come from the fact that the turbulent convection should be enchanced considerably in the inner layer by flow oscillation as shown in Chapter 3. At higher frequencies, it leads to increase the time-mean temperature in the inner layer and decrease in the outer layer although the amounts of change are not so appreciable.

In Fig. 5–15, the amplitude distributions of temperature oscillation in the boundary layer are shown. The temperature close to the cylinder oscillates with amplitudes approximately proportional to its time-mean. At further downstream points, the amplitude takes almost constant values in the inner layer. For larger values of H, its distribution has an approximately symmetric profile. Higher frequencies of velocity oscillation reduce the amplitude greatly in the inner layer rather than in the outer layer.

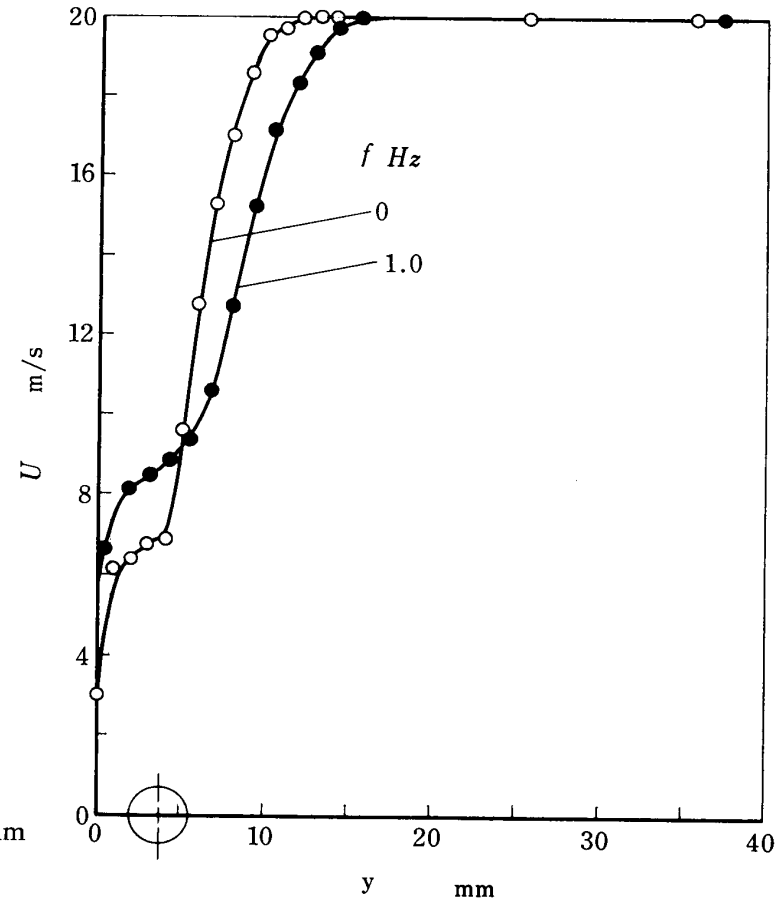

(a) H=3.8 mm

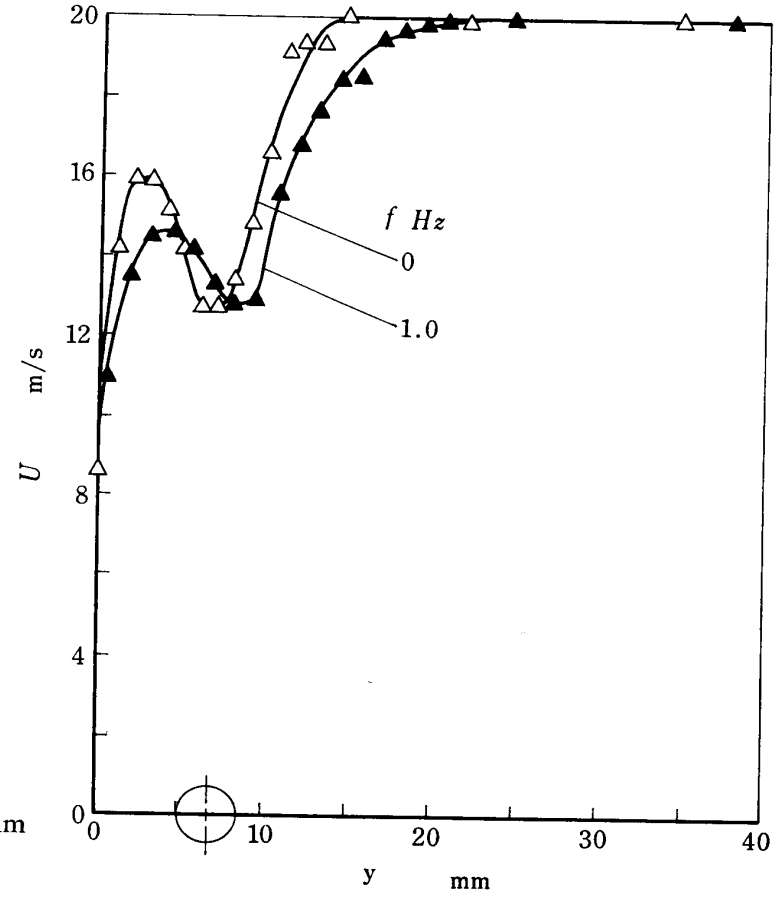

(b) H=6.8 mm

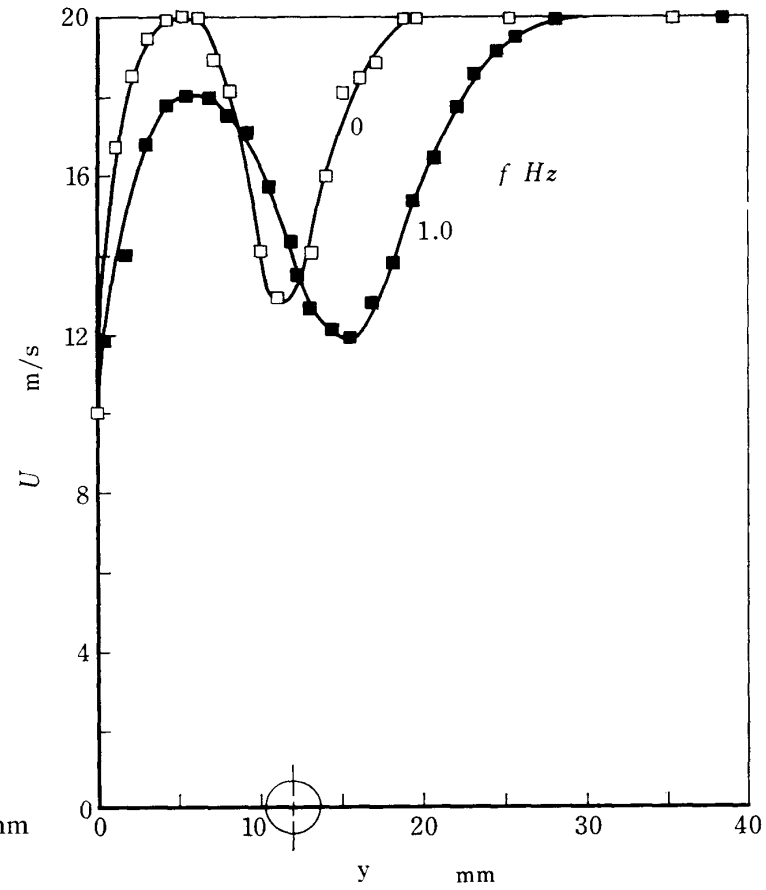

(c) H=11.8 mm

FIG. 5-12. Time-mean velocity distribution in the boundary layer of the plate behind the cylinder; $\bar{U}_\infty$=20 m/s, $\alpha_{u\infty}$=0.25, d=3.6 mm, x=30 mm, H=3.8 mm (a), 6.8 mm (b), 11.8 mm (c).

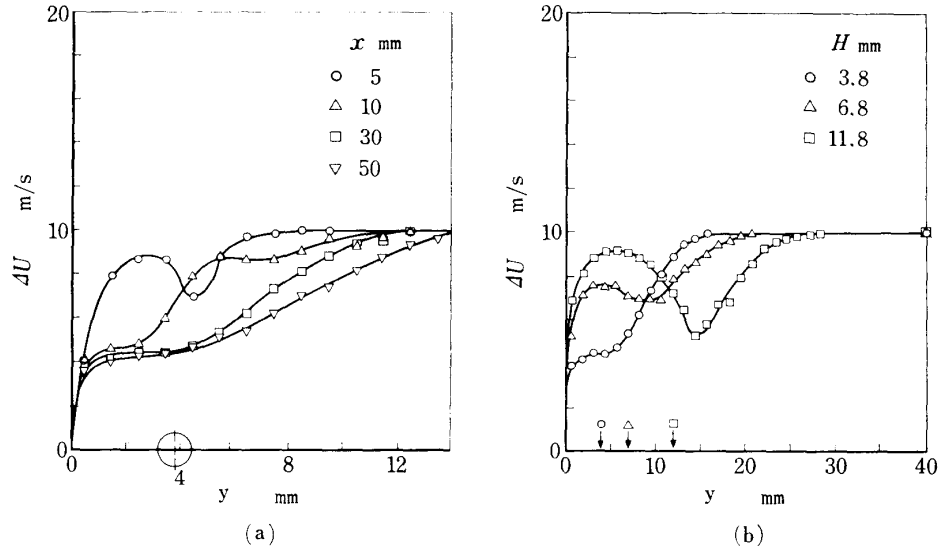

FIG. 5-13. Amplitude distribution of velocity oscillation in the bonndary layer of the plate behind the cylinder; $\bar{U}_\infty$=20 m/s, $\alpha_{u\infty}$=0.25, f=1.0 Hz, d=3.6 mm H=3.8 mm (a), x=30 mm (b).

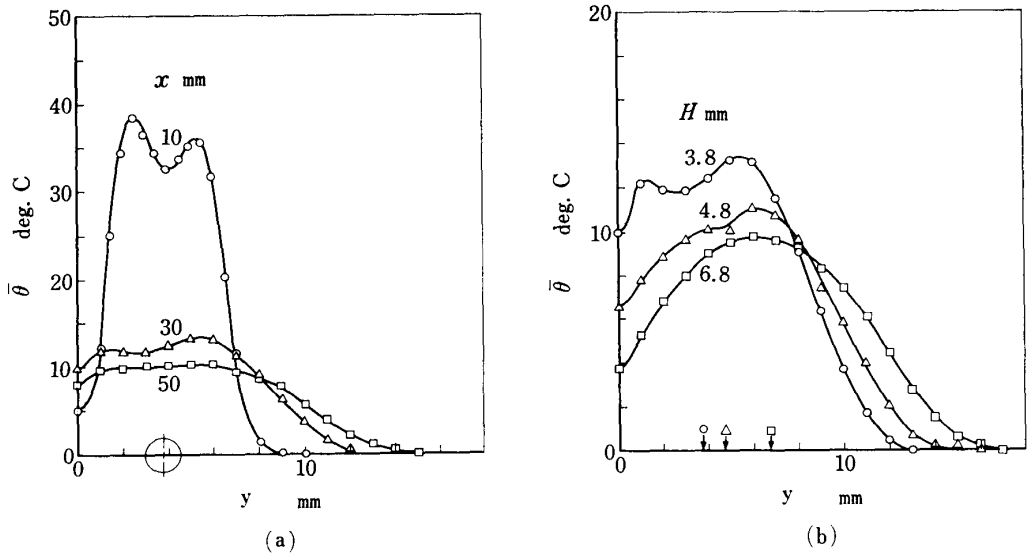

FIG. 5-14. Time-mean temperature distribution in the boundary layer of the plate behind the cylinder; $\overline{U}_\infty=20$ m/s, $\alpha_{u\infty}=0.25$, $f=1.0$ Hz, $d=3.6$ mm, $H=3.8$ mm(a), $x=30$ mm(b), $t_w=200$ μm, $q=1.9\times10^5$ kcal/m^{2}h.

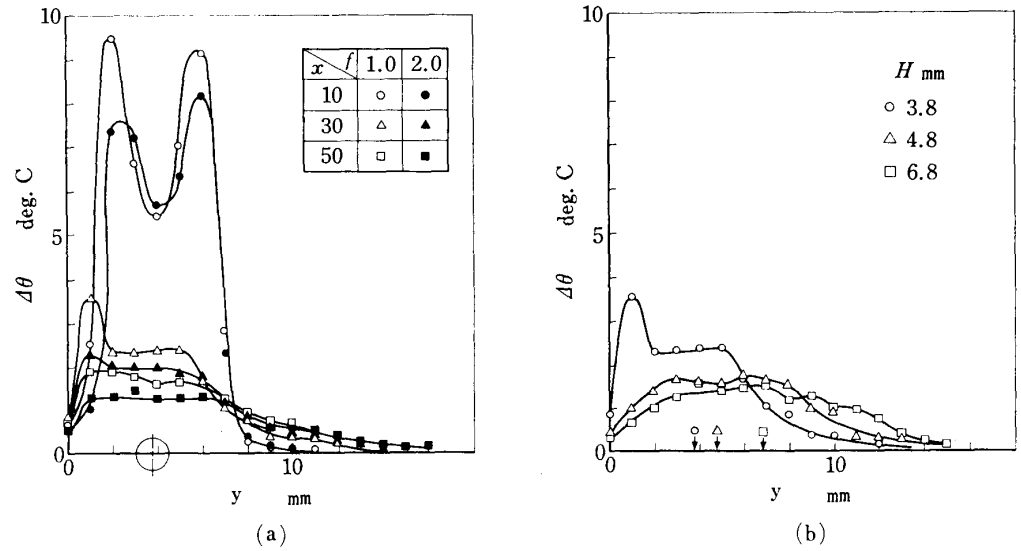

FIG. 5-15. Amplitude distribution of temperature oscillation in the boundary layer of the plate behind the cylinder; $\overline{U}_\infty=20$ m/s, $\alpha_{u\infty}=0.25$, $f=1.0$ Hz, $d=3.6$ mm, $H=3.8$ mm(a), $x=30$ mm(b), $t_w=200$ μm, $q=1.9\times10^5$ kcal/m^{2}h.

The surface temperatures of the flat plate are shown in Fig. 5-16. The frequency of velocity oscillation has little effect on the time-mean and amplitude of surface-temperature oscillation, slightly increasing the time-mean and slightly decreasing the amplitude. The time-mean takes two maxima and one minimum between the maxima. The first maximum and minimum may be attributed to the flow accelerated by the wake displacement between the cylinder and the plate. The amplitude also

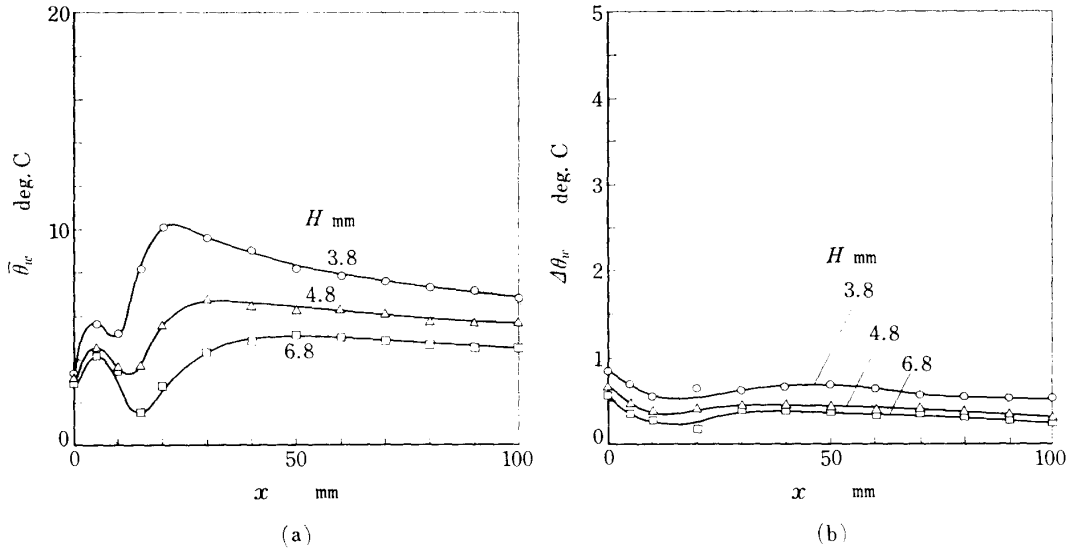

FIG. 5-16. Time-mean wall-temperature distribution along the plate; $\bar{U}_\infty=20$ m/s, $\alpha_{u\infty}=0.25$, $f=1.0$ Hz, $d=3.6$ mm, $t_w=200\,\mu$m, $q=1.9\times10^5$ kcal/m^{2}h.

takes a minimum at the minimum point of the time-mean temperature although it changes slightly through a large part of plate length.

6. CONCLUSION

The heat transfer characteristics of a plate, a cylinder and a cylinder above a plate located in sinusoidally oscillating flows with large amplitudes were investigated experimentally. The oncoming main stream of air was oscillated in the magnitude of velocity not in its direction, with a constant temperature. A thin stainless foil covered the surface of the cylinder or plate was heated electrically with a constant heat flux. By measuring the surface temperature of the foil heater, the response of the heat transfer, the amplitude and the phase, to the velocity oscillation of main flow was studied. The velocity and temperature fields in the vicinity of the cylinder and plate were also measured to study the heat transfer mechanism in oscillatory flows. In summary, the following results were obtained.

Flat plate

(1) Velocity distribution in the boundary layer; The time-mean velocity distribution is not affected by the frequency and amplitude of velocity oscillation of the main flow. The amplitude in the inner layer is increased at higher frequencies compared with that in the outer layer. The phase is uniform in phase throughout the layer. The turbulent intensities and the Reynolds stress are decreased in the inner layer and increased in the outer layer with increasing frequency.

(2) Temperature distribution in the boundary layer; No time-mean temperature difference is associated with the velocity oscillation of main flow. The amplitude takes a maximum value close to the plate-wall and decreases with increasing the frequency of velocity oscillation. The phase advances close to the plate wall and also advances from 180° lag to in-phase as the frequency increases.

(3) Wall-temperature along the plate; The time-mean wall-temperature, that is, the time-mean heat transfer coefficient is not affected by the velocity oscillation of the main flow. At higher frequencies, the amplitude is reduced greatly, and the phase advances to be in-phase with velocity oscillation.

Cylinder

(1) Wall-temperature along the cylinder; The time-mean temperature is increased in the separated region with increasing the frequency of velocity oscillation. The amplitude takes larger values in the separated region and smaller values in the vicinity of the separation point, being decreased rapidly throughout the surface at higher frequencies. The phase is rather uniform throughout the surface, becoming in-phase at higher frequencies.

(2) Heat transfer coefficient; The time-mean heat transfer coefficient deteriorates in the separated region. The amplitude of heat transfer coefficient is large both in the forward and rearward regions and small close to the separation point.

Cylinder above plate

(1) Wall-temperature of the cylinder; The time-mean wall-temperature of the cylinder tends to decrease at the points faced to the plate. The amplitude distribution is affected only through the change in the separation point which is shifted rearward with increasing frequency. The phase distribution is hardly affected by the velocity oscillation, being roughly uniform throughout the surface.

(2) Heat transfer coefficient of the cylinder; The overall heat transfer coefficient based on the time-mean temperature averaged over the wall-surface is hardly affected by the velocity oscillation. The amplitude of its oscillation increases proportionally to the amplitude of velocity oscillation and decreases inversely proportionally to the frequency, but is hardly affected by the cylinder location above the plate.

(3) Velocity and temperature distributions behind the cylinder in the boundary layer; The time-mean velocity and temperature distributions tend to be shifted toward the outer part of the boundary layer with the velocity oscillation, taking smaller values in the inner layer and larger values in the outer layer. Their amplitude distributions are also shifted and diffused toward the outer layer at higher frequencies, being decreased in the inner layer.

Department of Propulsion
Institute of Space and Aeronautical Science
University of Tokyo
10 December, 1980

References

[1] Lighthill, M. J., The response of laminar skin friction and heat transfer to fluctuations in the stream velocity, Proc. Roy. Soc. A224, 1–23 (1954).

[2] Kestin, J., Persen, L. N. and Shah, V. L., The transfer of heat across a two-dimensional, oscillating boundary layer, Z. Flugwiss. **15**, 277–285 (1967).

[3] Fortuna, O. and Hannatty, T. J., Frequency response of the boundary layer on wall transfer probes, Int. J. Heat Mass Transfer **14**, 1499–1507 (1971).

[4] Evans, N. A., Heat transfer through the unsteady laminar boundary layer on a semi-infinite flat plate. Part I: Theoretical considerations, Int. Heat Mass Transfer **16**, 555–565 (1973).
[5] Takhar, H. S. and Soundalgekar, V. M., Effects of viscous dissipation on heat transfer in an oscillating flow past a flat plate, Appl. Scient. Res. **33**, 101–111 (1977).
[6] Mori, Y., Imabayashi, M., Hijikata, K. and Yoshida, Y., Unsteady heat and mass transfer from spheres, Int. J. Heat Mass Transfer **12**, 571–585 (1969).
[7] Bayley, F. J., Edwards, P. A. and Singh, P. P., The effect of flow pulsations on heat transfer by forced convection from a flat plate, Proc. Int. Heat Transfer Conf. **59**, 499–509 (1961).
[8] Feilar, C. D. and Yeager, E. B., Effect of large amplitude oscillations on heat transfer, NASA TR R-142 (1962).
[9] Hatta, K., Kotake, S. and Aoki, I., Heat transfer in unsteady flows, Heat Transfer-Japanese Research 1-1, 1–10 (1972).

APPENDIX Heat transfer from a flat plate with a constant temperature in turbulent oscillating flows with small amplitudes.

The fluctuations in heat transfer from a flat plate located in laminar oscillating flows with small amplitude were considered by Lighthill [1] for the case of constant temperatures of both the plate and the oncoming flow. The heat transfer from a plate of constant temperature in the turbulent boundary layer can also be solved approximately in the similar manner.

The equation of energy in the boundary-layer approximation is given by

$$\frac{\partial\theta}{\partial t}+u\frac{\partial\theta}{\partial x}+v\frac{\partial\theta}{\partial y}=\frac{\partial}{\partial y}\left\{(\kappa+\kappa_t)\frac{\partial\theta}{\partial y}\right\}, \tag{A-1}$$

where x is measured along the wall-surface, y perpendically to the surface, and (u, v) are the corresponding velocities. κ and κ_t are the laminar and turbulent diffusivities of temperature. The boundary condition of the temperature field is given by

$$\begin{aligned} &\theta=\theta_w \qquad y=0 \quad x\geqslant 0,\\ &\theta=0 \qquad y=\infty \quad x\geqslant 0,\\ &\theta=0 \qquad x<0, \end{aligned} \tag{A-2}$$

where the plate surface is assumed to take a constant temperature θ_w $(=T_w-T_\infty)$.

Corresponding to the velocity oscillation in the main flow

$$U_\infty=\bar{U}_\infty(1+\alpha_{u\infty}e^{i\omega t}), \tag{A-3}$$

the velocity and temperature oscillations in the boundary layer are written as

$$\begin{aligned} U&=\bar{U}+U_1e^{i\omega t}\\ V&=\bar{V}+V_1e^{i\omega t}\\ \theta&=\bar{\theta}+\theta_1e^{i\omega t}. \end{aligned} \tag{A-4}$$

The magnitude of the amplitude of velocity oscillation in the main flow is now assumed to be small so that

$$\alpha_{u\infty}^2 \ll 1. \tag{A-5}$$

Hence, the associated velocity and temperature oscillations in the boundary layer have the amplitude of the order of

$$\left(\frac{U_1}{\bar{U}}\right)^2 \ll 1 \qquad \left(\frac{V_1}{\bar{V}}\right)^2 \ll 1 \qquad \left(\frac{\theta_1}{\bar{\theta}}\right)^2 \ll 1. \tag{A-6}$$

The terms which include the second order or higher of these oscillatory components can be neglected in the governing equations. Substituting Eq. (A-4) into Eq. (A-1) and retaining only the terms of order $\alpha_{u\infty}$ lead to

$$i\omega\theta_1+\bar{U}\frac{\partial\theta_1}{\partial x}+\bar{V}\frac{\partial\theta_1}{\partial y}+U_1\frac{\partial\bar{\theta}}{\partial x}+V_1\frac{\partial\bar{\theta}}{\partial y}=\frac{\partial}{\partial y}\left\{(\kappa+\kappa_t)\frac{\partial\theta_1}{\partial y}\right\}, \tag{A-7}$$

of which the boundary condition is

$$\begin{aligned}\theta_1&=0 \qquad y=0\\ \theta_1&=0 \qquad y=\infty.\end{aligned} \tag{A-8}$$

In order to consider the approximate solution for the cases of lower and higher frequencies of oscillation, it is convenient to write the oscillating terms as

$$\begin{aligned}U_1&=U_s+i\omega U^*\\ V_1&=V_s+i\omega V^*\\ \theta_1&=\theta_s+i\omega\theta^*,\end{aligned} \tag{A-9}$$

where U_s, V_s and θ_s imply the quasi-steady solutions in the limiting case $\omega\to 0$. The quasi-steady solutions are the coefficient of $\alpha_{u\infty}$ in the steady solutions with a main flow $\bar{U}_\infty(1+\alpha_{u\infty})$, that is,

$$U_s=\bar{U}_\infty\frac{\partial\bar{U}}{\partial\bar{U}_\infty} \qquad V_s=\bar{U}_\infty\frac{\partial\bar{V}}{\partial\bar{U}_\infty} \qquad \theta_s=\bar{U}_\infty\frac{\partial\bar{\theta}}{\partial\bar{U}_\infty}. \tag{A-10}$$

Since the steady solution is a function of y/δ where δ is the boundary layer thickness

$$\bar{U}=\bar{U}_\infty f_u\left(\frac{y}{\delta_u}\right) \qquad \bar{V}=\bar{U}_\infty f_v\left(\frac{y}{\delta_u}\right) \qquad \bar{\theta}=\bar{\theta}_w f_t\left(\frac{y}{\delta_t}\right), \tag{A-11}$$

the quasi-steady solutions are then

$$\begin{aligned}U_s&=\bar{U}_\infty f_u\cdot\left(1-\frac{y}{\delta_u}\frac{f_u'}{f_u}\frac{\bar{U}_\infty}{\delta_u}\frac{\partial\delta_u}{\partial\bar{U}_\infty}\right)\\ V_s&=\bar{U}_\infty f_v\cdot\left(1-\frac{y}{\delta_u}\frac{f_v'}{f_v}\frac{\bar{U}_\infty}{\delta_u}\frac{\partial\delta_u}{\partial\bar{U}_\infty}\right)\\ \theta_s&=-\bar{\theta}_w f_t'\cdot\frac{y}{\delta_u}\frac{\bar{U}_\infty}{\delta_u}\frac{\partial\delta_u}{\partial\bar{U}_\infty}, \qquad (f'\equiv\partial f(y)/\partial y).\end{aligned} \tag{A-12}$$

The quasi-steady solution of temperature θ_s is also a solution of Eq. (A-7) when $\omega \to 0$, that is

$$\bar{U}\frac{\partial\theta_s}{\partial x}+\bar{V}\frac{\partial\theta_s}{\partial y}+U_s\frac{\partial\bar{\theta}}{\partial x}+V_s\frac{\partial\bar{\theta}}{\partial y}=\frac{\partial}{\partial y}\left\{(\kappa+\kappa_t)\frac{\partial\theta_s}{\partial y}\right\}. \tag{A-13}$$

The frequency-dependent term, θ^*, is then given by solving the equation deduced from Eq. (A-7) with Eq. (A-13)

$$i\omega\theta^*+\bar{U}\frac{\partial\theta^*}{\partial x}+\bar{V}\frac{\partial\theta^*}{\partial y}-\frac{\partial}{\partial y}\left\{(\kappa+\kappa_t)\frac{\partial\theta^*}{\partial y}\right\}=-\theta_s-\left(U^*\frac{\partial\bar{\theta}}{\partial x}+V^*\frac{\partial\bar{\theta}}{\partial y}\right). \tag{A-14}$$

The first term on the right-hand side, $-\theta_s$, means the thermal inertial due to the quasi-steady temperature oscillation and the other terms represent the oscillatory heat fluxes due to oscillatory convection. The heat transfer rate at the wall is given by

$$-\lambda\left(\frac{\partial\theta}{\partial y}\right)_{y=0}=-\lambda\left(\frac{\partial\bar{\theta}}{\partial y}\right)_{y=0}-e^{i\omega t}\left\{\lambda\left(\frac{\partial\theta_s}{\partial y}\right)_{y=0}+i\omega\lambda\left(\frac{\partial\theta^*}{\partial y}\right)_{y=0}\right\}. \tag{A-15}$$

Lower-frequency approximate solution

Integrating Eq. (A-14) with respect to y over the whole boundary layer leads to

$$i\omega\int_0^\infty\theta^*dy+\frac{\partial}{\partial x}\int_0^\infty\bar{U}\theta^*dy+\kappa\left(\frac{\partial\theta^*}{\partial y}\right)_0=-\int_0^\infty\theta_s dy-\frac{\partial}{\partial x}\int_0^\infty U^*\bar{\theta}dy, \tag{A-16}$$

where the equation of continuity has been used. In Eq. (A-16), retaining the dominant terms when $\omega\to 0$ gives

$$\kappa\left(\frac{\partial\theta^*}{\partial y}\right)_{y=0}=-\int_0^\infty\theta_s dy. \tag{A-17}$$

Substituting Eq. (A-12) for θ_s into the integral on the right-hand gives

$$\int_0^\infty\theta_s dy=-\bar{\theta}_w\bar{U}_\infty\frac{\partial\delta_t}{\partial\bar{U}_\infty}\int_0^\infty\frac{y}{\delta_t}\frac{\partial(f_t-1)}{\partial(y/\delta_t)}d\left(\frac{y}{\delta_t}\right)=-\bar{\theta}_w\bar{U}_\infty\frac{\partial\delta_t}{\partial\bar{U}_\infty}. \tag{A-18}$$

The heat transfer rate is then

$$-\lambda\left(\frac{\partial\theta}{\partial y}\right)_{y=0}=-\lambda\left(\frac{\partial\bar{\theta}}{\partial y}\right)_{y=0}+e^{i\omega t}\frac{\bar{U}_\infty}{\delta_t}\frac{\partial\delta_t}{\partial\bar{U}_\infty}\left\{\lambda\left(\frac{\partial\bar{\theta}}{\partial y}\right)_0-i\omega\frac{\lambda}{\kappa}\delta_t\bar{\theta}_w\right\}. \tag{A-19}$$

The phase is always behind that of velocity oscillation, being proportional to the frequency. It should be noted that in the present experimental result the phase of heat transfer rate lags in a similar way with increasing the frequency.

Higher-frequency approximate solution

The dominant terms of Eq. (A-7) for large ω gives

$$\frac{\partial}{\partial y}\left\{(\kappa+\kappa_t)\frac{\partial\theta_1}{\partial y}\right\}-i\omega\theta_1=U_1\frac{\partial\bar{\theta}}{\partial x}+V_1\frac{\partial\bar{\theta}}{\partial y}. \tag{A-20}$$

Corresponding to Eq. (A-20), equation of motion can be expressed as

$$\frac{\partial}{\partial y}\left\{(\nu+\nu_t)\frac{\partial U_1}{\partial y}\right\}-i\omega U_1=0, \tag{A-21}$$

where ν and ν_t are the laminar and turbulent kinematic viscosities, respectively. Close to the wall, the turbulent difusivities κ_t and ν_t are assumed as

$$\kappa_t\simeq\kappa_0 y \qquad \nu_t\simeq\nu_0 y, \tag{A-22}$$

although more exactly they are proportional to y^3 or y^4. Then, the approximations of Eqs. (A-20) and (A-21) are

$$(\kappa+\kappa_0 y)\frac{\partial^2\theta_1}{\partial y^2}-i\omega\theta_1=U_1\frac{\partial\bar{\theta}}{\partial x}+V_1\frac{\partial\bar{\theta}}{\partial y} \tag{A-23}$$

$$(\nu+\nu_0 y)\frac{\partial^2 U_1}{\partial y^2}-i\omega U_1=0 \tag{A-24}$$

The solution of Eq. (A-24) is given by

$$\begin{aligned} U_1&=\bar{U}_\infty\left\{1-\sqrt{z}\,\frac{H_1^{(2)}(\sqrt{\alpha z})}{H_1^{(2)}(\sqrt{\alpha})}\right\}\\ &\simeq\bar{U}_\infty\{1-z^{1/4}e^{-i\sqrt{\alpha}(\sqrt{z}-1)}\}, \end{aligned} \tag{A-25}$$

where $H_1^{(2)}$ is the Hankel function of the second kind of order one and

$$z\equiv\frac{\nu+\nu_0 y}{\nu} \qquad \alpha\equiv-\frac{4\nu\omega}{\nu_0^2}i.$$

Substituting Eq. (A-25) into Eq. (A-23) and assuming $\bar{\theta}\simeq\theta_w+y(\partial\bar{\theta}/\partial y)_0$ lead to

$$z\frac{\partial^2\theta_1}{\partial z^2}+\frac{\alpha}{4}\theta_1\simeq\left(\frac{\partial^2\bar{\theta}}{\partial x\partial y}\right)_{y=0}\frac{\nu^2\bar{U}_\infty}{\nu_0^3}(z-1)\{1-e^{-i\sqrt{\alpha}(\sqrt{z}-1)}\}, \tag{A-26}$$

where for simplicity $\kappa=\nu$ and $\kappa_0=\nu_0$ are assumed. The solution of Eq. (A-26) is given by

$$\theta_1=\sqrt{z}\,H_1^{(1)}(\sqrt{\alpha z})\left\{\int_1^z W_1dz+C_1\right\}+\sqrt{z}\,H_1^{(2)}(\sqrt{\alpha z})\left\{\int_0^z W_2dz+C_2\right\} \tag{A-27}$$

where $H^{(1)}$ and $H^{(2)}$ are the Hankel functions of the first and second kind, respectively and W_1 and W_2 are

$$\begin{aligned} W_1&=-\frac{i\pi}{\sqrt{\alpha}}\left(\frac{\partial^2\bar{\theta}}{\partial x\partial y}\right)_{y=0}\frac{\nu^2\bar{U}_\infty}{\nu_0^3}(z-1)\{1-e^{-i\sqrt{\alpha}(\sqrt{z}-1)}\}H_1^{(2)}(\sqrt{\alpha z})\\ W_2&=\frac{i\pi}{\alpha}\left(\frac{\partial^2\bar{\theta}}{\partial x\partial y}\right)_{y=0}\frac{\nu^2\bar{U}_\infty}{\nu_0^3}(z-1)\{1-e^{-i\sqrt{\alpha}(\sqrt{z}-1)}\}H_1^{(1)}(\sqrt{\alpha z}). \end{aligned}$$

The integral constants C_1 and C_2 are determined by the boundary condition $\theta_1=0$ at

$y=0$ and $y=\infty$. Finally, Eq. (A-27) with $\omega\to\infty$ becomes

$$\theta_1=\frac{2i}{\sqrt{\alpha}}\left(\frac{\partial^2\bar{\theta}}{\partial x\partial y}\right)_{y=0}\frac{\nu^2\bar{U}_\infty}{\nu_0^3}\sqrt{z}\left\{\left(\frac{2}{7}z-\frac{2}{3}\right)e^{-i\sqrt{\alpha}(\sqrt{z}-1)}+\frac{8}{21}\frac{H_1^{(2)}(\sqrt{\alpha z})}{H_1^{(2)}(\sqrt{\alpha})}\right\} \quad \text{(A-28)}$$

Then, the heat transfer rate is

$$-\lambda\left(\frac{\partial\theta}{\partial y}\right)_{y=0}=-\lambda\left(\frac{\partial\bar{\theta}}{\partial y}\right)_{y=0}-e^{i\omega t}\frac{4}{21}\frac{\nu\bar{U}_\infty}{\nu_0^2}\sqrt{\frac{\nu_0^2}{\nu\omega}}\left(\frac{\partial^2\bar{\theta}}{\partial x\partial y}\right)_{y=0}e^{-i\pi/4}. \quad \text{(A-29)}$$

Since $(\partial^2\bar{\theta}/\partial x\partial y)_{y=0}$, is negative, the phase of the heat transfer rate at higher frequencies is behind that of velocity oscillation by 90°. This is in contrast to the experimental case in which the heat transfer rate lags approximately by 180° at higher frequencies.